

NEW ORTHOGONAL SPACE-TIME BLOCK CODES WITH FULL DIVERSITY

A Thesis

by

LORI ANNE DALTON

Submitted to the Office of Graduate Studies of  
Texas A&M University  
in partial fulfillment of the requirements for the degree of

MASTER OF SCIENCE

December 2002

Major Subject: Electrical Engineering

NEW ORTHOGONAL SPACE-TIME BLOCK CODES WITH FULL DIVERSITY

A Thesis

by

LORI ANNE DALTON

Submitted to Texas A&M University  
in partial fulfillment of the requirements  
for the degree of

MASTER OF SCIENCE

Approved as to style and content by:

---

Costas N. Georghiades  
(Chair of Committee)

---

Scott L. Miller  
(Member)

---

Chin B. Su  
(Member)

---

Marina Vannucci  
(Member)

---

Chanan Singh  
(Head of Department)

December 2002

Major Subject: Electrical Engineering

## ABSTRACT

New Orthogonal Space-Time Block Codes with Full Diversity. (December 2002)

Lori Anne Dalton, B.S., Texas A&M University

Chair of Advisory Committee: Dr. Costas N. Georghiades

It has been shown from the Hurwitz-Radon theorem that square complex orthogonal space-time code designs cannot achieve full diversity and full rate simultaneously, except in the two transmit antenna case. However, this result does not consider non-linear codes, or codes that only exist for specific symbol constellation sets. In this work, we present complex full rate codes for four transmit antennas. Using carefully tailored constellation phase rotations, we show these codes can achieve full diversity for specialized PSK and PAM symbol constellations. In addition, one code presented with PAM based symbols is a linear complex orthogonal design. Thus, we demonstrate by example that full rate, full diversity, square complex orthogonal codes for four transmit antennas exist when symbol constellations are restricted to a subset of the complex plane. This new code does not violate the Hurwitz-Radon theorem, which only considers codes that work for all possible symbol constellations.

To my wonderful parents, Scott and Tahnee, and my terrific little brother, Maxim

## ACKNOWLEDGMENTS

I would first like to thank my advisor, Dr. Costas Georghiades, for introducing me to wireless communications and space-time coding. He has been an excellent guide in my transition from undergraduate school to graduate school. I also thank my other committee members, Dr. Scott Miller, Dr. Chin Su, and Dr. Marina Vannucci, for their valuable comments and for committing their time to help me with this work. Thanks also to the remaining professors of the wireless communications group: Dr. Krishna Narayanan, Dr. Zixiang Xiong, Dr. Erchin Serpedin, and Dr. Xiaodong Wang (now at Columbia University), for their input and support.

I could not be where I am today without the unconditional love and encouragement of my parents and brother. I thank my Mom and brother particularly for their emotional and spiritual support. Without them, my life would not be complete. Finally, I thank my Dad for continually stimulating my mind and inspiring my interest in engineering, math, and science. I remember fondly my very first lesson on numbers from him.

## TABLE OF CONTENTS

CHAPTER		Page
I	INTRODUCTION . . . . .	1
	A. Introduction to the Wireless Problem . . . . .	1
	B. Introduction to Space-Time Coding . . . . .	2
	1. Notation . . . . .	3
	2. Channel Model . . . . .	4
	3. The Code Matrix . . . . .	5
	C. Benefits of Space-Time Coding . . . . .	5
	1. Improved Performance with Diversity . . . . .	5
	2. Higher Data Rate, Capacity, and Spectral Efficiency . . . . .	7
	3. Simpler Handheld Design . . . . .	9
	D. Orthogonal Code Matrix Design . . . . .	9
	E. Literature Review . . . . .	13
II	A CLASS I NON-LINEAR ORTHOGONAL CODE . . . . .	15
	A. An Example: The Alamouti Code . . . . .	15
	B. An Example: STTD-OTD . . . . .	16
	C. The New Code Matrix . . . . .	18
	D. Linearity . . . . .	19
	E. Diversity Analysis . . . . .	19
III	A CLASS II NON-LINEAR ORTHOGONAL CODE . . . . .	21
	A. The New Code Matrix . . . . .	22
	B. Linearity . . . . .	24
	C. Diversity Analysis . . . . .	25
	D. Constellation Design . . . . .	26
	1. PAM Based Constellations . . . . .	26
	2. PSK Based Constellations . . . . .	27
	E. Capacity . . . . .	28

CHAPTER	Page
F. Receivers for Known Fading . . . . .	31
1. Optimal Receivers . . . . .	31
a. Using PAM Base Constellations . . . . .	34
b. Using PSK Base Constellations . . . . .	35
2. Sub-Optimal Receivers . . . . .	35
G. Receivers for Unknown Known Fading . . . . .	36
IV PERFORMANCE . . . . .	39
A. Class I Non-Linear Code Performance . . . . .	40
1. Non-Rotated QPSK Constellations . . . . .	40
2. Rotated QPSK Constellations . . . . .	41
B. Class II Non-linear Code Performance . . . . .	42
1. Rotated 4-PAM Constellations . . . . .	42
2. Rotated QPSK Constellations and Linear Receiver . .	43
3. Rotated QPSK Constellations and ML Receiver . . . .	44
4. Rotated BPSK Constellations and Unknown Fading .	45
V CONCLUSION . . . . .	47
A. Summary of Results . . . . .	47
B. Future Work . . . . .	48
REFERENCES . . . . .	49
APPENDIX A . . . . .	53
VITA . . . . .	56

## LIST OF TABLES

TABLE	Page
I “Bad” matrices for the class I non-linear code with QPSK symbols, phase shifted by $[0, 1, 2, 3] \pi/16$ . . . . .	54

## LIST OF FIGURES

FIGURE	Page
1	A typical communication system utilizing space-time coding. . . . . 3
2	Capacity of various $(N_t, N_r = N_t)$ systems. . . . . 8
3	(a) Constellations for PAM base symbols; (b) Resulting QAM transmit constellation. . . . . 27
4	(a) Constellations for QPSK base symbols; (b) Resulting transmit constellation. . . . . 29
5	Diversity product of the class II non-linear code with QPSK base symbols; $d_2$ and $d_4$ are rotated by $\phi$ with respect to $d_1$ and $d_3$ . . . . . 30
6	Capacity of the class II non-linear orthogonal code. . . . . 32
7	ML performance of the class I non-linear code with QPSK base symbols and no phase shifts. . . . . 40
8	ML performance of the class I non-linear code with QPSK symbols and phase shifts $[0, 0, 32, 19] \pi/128$ . . . . . 41
9	ML performance of the orthogonal code with 4PAM base symbols and phase shifts $[0, 1, 0, 1] \pi/2$ . . . . . 42
10	ZF and linear MMSE performance of the class II non-linear code with QPSK base symbols and phase shifts $[0, 1, 0, 1] \pi/4$ . . . . . 43
11	ML performance of the class II non-linear code with QPSK base symbols and phase shifts $[0, 1, 0, 1] \pi/4$ . . . . . 44
12	Sub-optimal performance in unknown fading ( $f_m T = 0$ ) of the class II non-linear code with BPSK base symbols and phase shifts $[0, 1, 0, 1] \pi/2$ . . . . . 46
13	QPSK symbol constellations with phase shifts $[0, 1, 2, 3] \pi/16$ . . . . . 55

## CHAPTER I

### INTRODUCTION

We first describe the wireless problem in Section A and present an introduction to space-time coding in Section B. In Section C, benefits of space-time coding are covered, followed by a discussion on orthogonal code design in Section D. In the latter section, we define two classes of “non-linear” orthogonal codes. Finally, a review of literature relevant to space-time block code design is presented in Section E.

#### A. Introduction to the Wireless Problem

Due to an explosion of demand for high-speed wireless services, such as wireless Internet, email, stock quotes, and cellular video conferencing, wireless communications has become one of the most exciting fields in modern engineering. However, development of such products and services poses a serious challenge: how can we support the exceedingly high data rates and capacity required for these applications with the severely restricted resources offered in a wireless channel?

The obstacles associated with wireless environments are difficult to overcome. Interference from other users and inter-symbol interference (ISI) from multiple paths of one’s own signal are serious forms of distortion [1], the latter effectively causing frequency-selective channel properties. Furthermore, when transmit and receive antennas are in relative motion, the Doppler effect will spread the frequency spectrum of received signals [2]. This results in time varying channel characteristics. Many systems must function without a line-of-sight (LOS) path between transmit and receive antennas, thus pure Rayleigh fading may completely attenuate a signal at times and

---

The journal model is *IEEE Transactions on Automatic Control*.

render a channel temporarily useless. Additionally, the usual additive white Gaussian noise (AWGN) corrupts the signal.

Besides the above difficulties, there are extremely limited bandwidth and stringent power limitations on both the mobile unit (for battery conservation) and the base station (to satisfy government safety regulations). To conserve bandwidth resources, we maximize spectral efficiency by packing as much information as possible into a given bandwidth. A solution to the bandwidth and power problem is the cellular concept, in which frequency bands are allocated to small, low power cells and reused at cells far away. However, this idea alone is not enough. We must look to other means, such as space-time coding, to increase data rate, capacity, and spectral efficiency.

## B. Introduction to Space-Time Coding

A typical communication system consists of a transmitter, a channel, and a receiver. Space-time coding involves use of multiple transmit and receive antennas, as illustrated in Fig. 1. Bits entering the space-time encoder serially are distributed to parallel sub-streams. Within each sub-stream, bits are mapped to signal waveforms, which are then emitted from the antenna corresponding to that sub-stream. The scheme used to map bits to signals is called a space-time code. Signals transmitted simultaneously over each antenna interfere with each other as they propagate through the wireless channel. Meanwhile, the fading channel also distorts the signal waveforms. At the receiver, the distorted and superimposed waveforms detected by each receive antenna are used to estimate the original data bits.

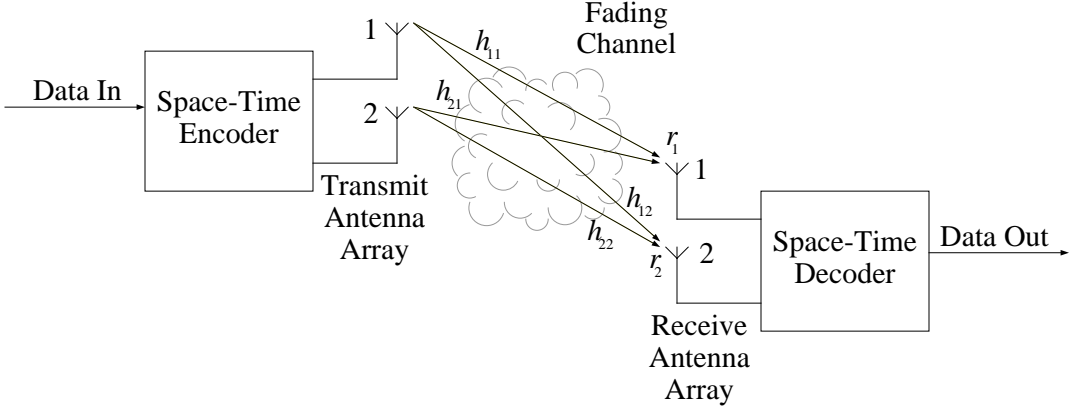


Fig. 1. A typical communication system utilizing space-time coding.

### 1. Notation

The following notation is used throughout this thesis.

- $j = \sqrt{-1}$ .
- $x^*$  is the complex conjugate of  $x$ .
- $\Re(x)$  is the real part of  $x$ .
- $\angle x$  is the phase of  $x$ .
- $E[X]$  is the expected value of random variable  $X$ .
- $\mathbf{X}^T$  is the transpose of matrix  $\mathbf{X}$ .
- $\mathbf{X}^H$  is the conjugate transpose of matrix  $\mathbf{X}$ .
- $\mathbf{I}_n$  is the  $n \times n$  identity matrix.
- $\mathbf{0}_n$  is the  $n \times n$  zero matrix.

## 2. Channel Model

In a space-time system, define  $N_t$  to be the number transmit antennas and  $N_r$  the number of receive antennas. Furthermore, assume we use a block coded system in which  $L2^M$  bits enter the encoder every block epoch. These bits are mapped to  $L$  symbols, each with an  $M$ -ary sized constellation, and transmitted over a block of  $T$  time intervals. We say this is an  $(N_t, N_r)$  block coded system with rate  $R = L/T$ . A mathematical model for any space-time block coded system is given by

$$\mathbf{R} = \mathbf{S} \cdot \mathbf{H} + \mathbf{N}, \quad (1.1)$$

where

- $\mathbf{R}$  is a  $T \times N_r$  matrix representing the received data.
- $\mathbf{S}$  is a  $T \times N_t$  matrix representing the transmitted symbols.
- $\mathbf{H}$  is an  $N_t \times N_r$  matrix representing quasi-static flat Gaussian fading.
- $\mathbf{N}$  is a  $T \times N_r$  matrix representing AWGN.

In the channel model (1.1), we only consider fading and AWGN distortion. Elements of the AWGN matrix,  $\mathbf{N}$ , are modeled as independent circularly symmetric (i.e., real and imaginary parts are independent) complex Gaussian random variables with zero mean, and a variance that defines the system signal-to-noise ratio (SNR).

The fading matrix,  $\mathbf{H}$ , is modeled in the same statistical manner as AWGN with normalized unit variance [1], [2]. A quasi-static channel remains constant over the duration of a code block, but changes independently from one block to another. Flat fading implies a constant power spectral density (PSD) over the frequency band used by the transmitted symbols [2]. We assume all antennas in the system are placed sufficiently far apart for independent fading over each channel.

### 3. The Code Matrix

Elements of code matrix  $\mathbf{S}$  are typically complex baseband symbols from a PSK or QAM constellation. A given column of  $\mathbf{S}$  represents the stream of data sent by a specific transmit antenna, while a given row represents the information sent in a single time interval. This structure in the code matrix gives the name, “space-time coding.” The average energy transmitted in each space-time code block satisfies  $E[\text{trace}(\mathbf{S}\mathbf{S}^H)] = TN_tE$ , where  $E$  is the average complex baseband symbol energy.

#### C. Benefits of Space-Time Coding

##### 1. Improved Performance with Diversity

Space-time coding can improve performance through an effect known as *diversity*. Diversity is a measure of the average number of channels fully utilized by each piece of information transmitted. The maximum diversity available to a space-time system is  $N_tN_r$ , which is the total number of channels between the transmitter and receiver.

When adding new antennas to a system, the receiver can use the extra channels to improve the probability of correctly identifying the true transmitted signal. We may view the new channels as redundancy, or backup in case other channels fail. For example, suppose we have one transmit and two receive antennas, and that one of the channels goes into a deep fade and is basically unusable. In this case, the other channel may still be able to recover the data. While both channels might fail simultaneously, this is highly unlikely compared to the event of a single channel failure. This is demonstrated by the following property of independent events.

$$\begin{aligned} & \Pr(\text{“channel 1 fails” and “channel 2 fails”}) \\ &= \Pr(\text{“channel 1 fails”}) \Pr(\text{“channel 2 fails”}). \end{aligned}$$

In this way, space-time coding offers the possibility of lower error probability.

Diversity in a fading channel can be directly determined from error probability. Specifically, the diversity of a system is given by the error probability behavior as  $\text{SNR} \rightarrow \infty$ , i.e.,

$$\Pr(\text{error}) = K\rho^{-D},$$

where  $D$  is the diversity order,  $\rho$  is the SNR, and  $K$  is a coding gain constant. Thus, performance plots on a log scale with SNR in dB approach a linear asymptote with slope  $-D$ .

In [4], the rank criterion was developed to determine the diversity order achieved by space-time codes. Essentially, it states  $D = NN_r$ , where  $N$  is the minimum rank of the difference between any two distinct code matrices,  $\mathbf{S} - \tilde{\mathbf{S}}$ . For a full diversity code,  $N = N_t$ . A necessary, but insufficient, condition for full diversity is that each symbol must be transmitted over every antenna. Another performance criterion is the determinant criterion, which addresses coding gain. For full diversity schemes, it simply maximizes the minimum determinant of  $\mathbf{S} - \tilde{\mathbf{S}}$ .

For square code matrices, one measure of the quality of a space-time code is the diversity product [5], given by

$$\zeta_v = \frac{1}{2} \min_{\mathbf{S} \neq \tilde{\mathbf{S}} \in V} \left| \det(\mathbf{S} - \tilde{\mathbf{S}}) \right|^{\frac{1}{N_t}}, \quad (1.2)$$

where  $V$  is the set of all data matrices  $\mathbf{S}$ . We observe  $\zeta_v$  is a measure of minimum distance. Some properties of the diversity product are listed below.

- $0 \leq \zeta_v \leq \sqrt{N_t E}$ .
- Any constellation with  $\zeta_v > 0$  achieves full diversity (from the rank criterion).
- Larger  $\zeta_v$  typically indicates a better code (from the determinant criterion).

## 2. Higher Data Rate, Capacity, and Spectral Efficiency

In general, the data rate of a space-time block code is defined to be the average number of symbols sent per time epoch, or simply  $R = L/T$ . A space-time code is full rate if  $L = T$ . The spectral efficiency of a modulation scheme is given by

$$\eta = \frac{\text{Data Rate}}{\text{Bandwidth}}.$$

We define the spectral efficiency of a space-time code using a two-dimensional constellation with  $M$  points to be  $\eta = R \log_2 M$  bits/sec/Hz.

Improved performance from diversity may be used to attain higher data rates by increasing the symbol constellation size. Since  $M$ -PSK and  $M$ -QAM modulations are bandwidth efficient signaling schemes (they use a fixed amount of bandwidth for any  $M$ ), space-time coding enables us to achieve higher levels of spectral efficiency at a fixed bandwidth and error rate.

It has been shown in [6] and [7] that space-time codes can achieve phenomenal capacity compared to traditional single transmit and receive antenna systems. In general, the capacity of a multi-input multi-output (MIMO) channel with Gaussian fading is

$$C = E_{\mathbf{H}} \left[ \log \det \left( \mathbf{I}_{N_r} + \frac{\rho}{N_t} \mathbf{H}^H \mathbf{H} \right) \right] \quad (1.3)$$

$$= E_{\mathbf{H}} \left[ \log \det \left( \mathbf{I}_{N_t} + \frac{\rho}{N_t} \mathbf{H} \mathbf{H}^H \right) \right], \quad (1.4)$$

where  $\rho$  is the SNR. A plot of capacity is illustrated in Fig. 2 for various systems with  $N_r = N_t$  receive antennas. Notice as the number of antennas is increased that capacity increases significantly. BLAST [8] is a space-time coding technique designed to achieve capacity and maximize data rate.

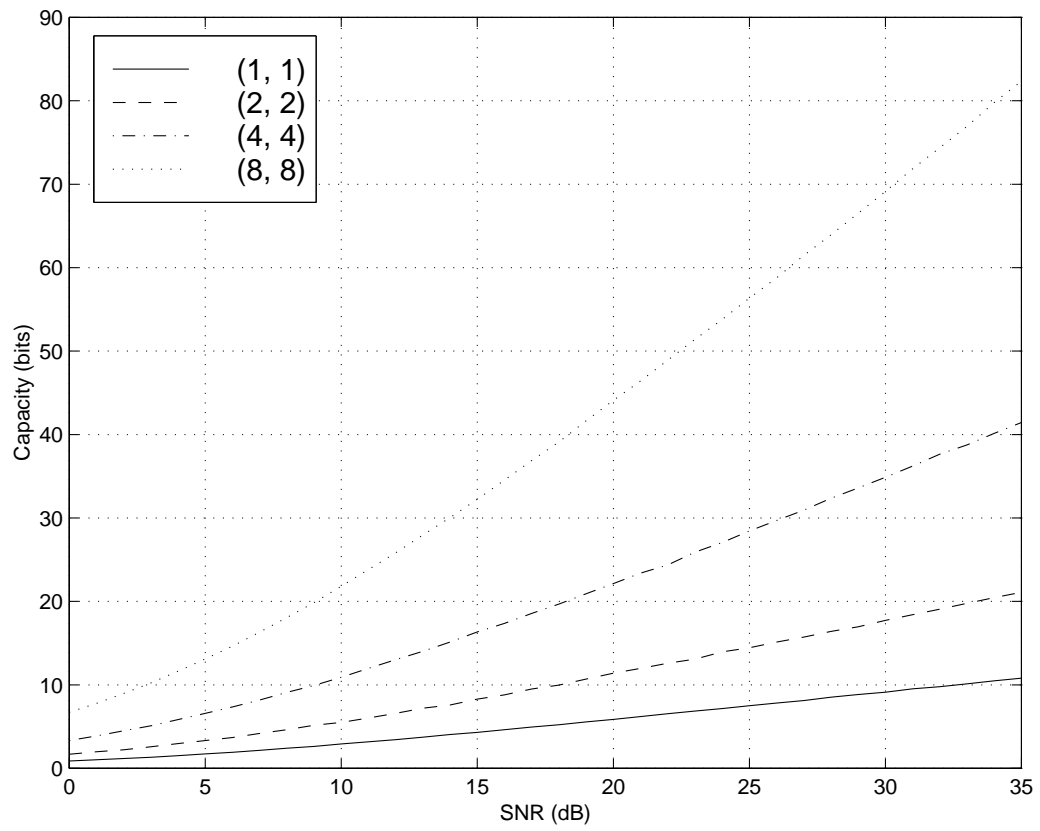


Fig. 2. Capacity of various  $(N_t, N_r = N_t)$  systems.

### 3. Simpler Handheld Design

We can achieve the same diversity effects with multiple antennas at the transmitter as with multiple antennas at the receiver. Thus, transmit diversity is appealing in systems with multiple information recipients, such as broadcast and cellular schemes. This is because we can increase diversity in all subscriber units by adding just one antenna to the base station, instead of a new antenna to each individual receiving unit, thus reducing the cost and complexity of each handheld device.

#### D. Orthogonal Code Matrix Design

Currently, there is interest in designing codes for 4 or more transmit antennas. Most space-time block codes in the literature are motivated by one or more of the following desirable properties: full diversity, full rate, simple maximum-likelihood (ML) detection, and minimum delay (i.e., a square code matrix).

Orthogonal codes are most remarkable for having simple ML receivers that decouple the symbols. In [3], several classes of full diversity orthogonal designs were defined. All of these codes (listed below) require  $\mathbf{S}^H \mathbf{S} = \mathbf{D}_{N_t}^1$ , where  $\mathbf{D}_{N_t}$  is a diagonal matrix whose diagonal elements are real linear combinations of the symbol energies,  $|s_i|^2$ ,  $i = 1, \dots, L$ .<sup>2</sup>

- Real orthogonal designs: an  $N_t \times N_t$  matrix with real entries  $\pm s_i$ ,  $i = 1, \dots, N_t$ .
- Complex orthogonal designs: an  $N_t \times N_t$  matrix with complex entries  $\pm s_i$ ,  $\pm s_i^*$ ,  $\pm j s_i$ , and  $\pm j s_i^*$ ,  $i = 1, \dots, N_t$ .

---

<sup>1</sup>This condition essentially requires the symbol streams transmitted by each antenna to be orthogonal to each other. Note for real designs  $\mathbf{S}^H \mathbf{S} = \mathbf{S}^T \mathbf{S}$ .

<sup>2</sup>An orthogonal code has full diversity if these linear combination coefficients are strictly positive.

- Real linear processing orthogonal designs: an  $N_t \times N_t$  matrix with real linear combinations of  $s_i$ ,  $i = 1, \dots, N_t$ , as entries.
- Complex linear processing orthogonal designs: an  $N_t \times N_t$  matrix with complex linear combinations of  $s_i$  and  $s_i^*$ ,  $i = 1, \dots, N_t$ , as entries.
- Generalized real orthogonal designs: a  $T \times N_t$  matrix with entries 0 or  $\pm s_i$ ,  $i = 1, \dots, L$ .
- Generalized complex orthogonal designs: a  $T \times N_t$  matrix with entries 0,  $\pm s_i$ ,  $\pm s_i^*$ ,  $\pm j s_i$ , and  $\pm j s_i^*$ ,  $i = 1, \dots, L$ .

It was shown in [3] that full diversity orthogonal designs exist if and only if a code exists such such that

$$\mathbf{S}^H \mathbf{S} = \frac{T}{L} (|s_1|^2 + |s_2|^2 + \dots + |s_L|^2) \mathbf{I}_{N_t}. \quad (1.5)$$

For an orthogonal code satisfying (1.5) with equal energy symbols,  $\mathbf{S}$  is a scaled unitary matrix, i.e.,  $\mathbf{S}^H \mathbf{S} = T E \mathbf{I}_{N_t}$ . For a square code matrix ( $T = N_t$ ), the criterion  $\mathbf{S}^H \mathbf{S} = T E \mathbf{I}_{N_t}$  is equivalent to  $\mathbf{S} \mathbf{S}^H = T E \mathbf{I}_T$ . However, for  $T > N_t$ , the ranks of  $\mathbf{S}^H \mathbf{S}$  and  $\mathbf{S} \mathbf{S}^H$  should be the same, and thus  $\mathbf{S} \mathbf{S}^H = T E \mathbf{I}_T$  does not hold. For  $T < N_t$ ,  $\mathbf{S}^H \mathbf{S} = T E \mathbf{I}_{N_t}$  is not possible.

Consider code matrices containing only linear combinations of the data symbols. We may set the  $i^{\text{th}}$  column of  $\mathbf{S}$  to  $\mathbf{B}_i \mathbf{X}^T$ , where  $\mathbf{X}$  is a row vector of the  $L = T$  real symbols transmitted in a block, and the  $\mathbf{B}_i$  are arbitrary  $L \times L$  real matrices. To construct generalized ( $T \geq N_t$ ) full rate, full diversity real orthogonal designs,  $\mathbf{B}_i$  must satisfy,

$$\mathbf{B}_i \mathbf{B}_i^T = \mathbf{B}_i^T \mathbf{B}_i = \mathbf{I}_L, \quad 1 \leq i \leq N_t, \quad (1.6)$$

$$\mathbf{B}_i^T \mathbf{B}_j = -\mathbf{B}_j^T \mathbf{B}_i, \quad 1 \leq i, j \leq N_t. \quad (1.7)$$

Let  $\mathbf{A}_j = \mathbf{B}_1^T \mathbf{B}_j$ , for  $j = 1, \dots, N_t$  (note  $\mathbf{A}_1 = \mathbf{I}_{N_t}$ ). Then the criteria (1.6) and (1.7) become:

$$\mathbf{A}_i^T \mathbf{A}_i = \mathbf{I}_L, \quad 2 \leq i \leq N_t, \quad (1.8)$$

$$\mathbf{A}_i^T = -\mathbf{A}_i, \quad 2 \leq i \leq N_t, \quad (1.9)$$

$$\mathbf{A}_i \mathbf{A}_j = -\mathbf{A}_j \mathbf{A}_i, \quad 2 \leq i, j \leq N_t. \quad (1.10)$$

These conditions define a size  $N_t - 1$  family of  $L \times L$  Hurwitz-Radon matrices. It was shown in [3] that a size  $k$  Hurwitz-Radon family of  $n \times n$  matrices is limited in size by  $k \leq n - 1$ , and that equality is only possible for  $n = 2, 4$ , or  $8$ . Applying this mathematical result to orthogonal designs, we discover that real full rate and full diversity square orthogonal designs ( $N_t = L = T$ ) only exist for  $N_t = 2, 4$ , or  $8$ .

Define  $A(R, N_t)$  to be the minimum  $T$  such that a  $T \times N_t$  real orthogonal code matrix exists with at least rate  $R$ . For full rate codes ( $R = 1$ ), this is equivalent to the minimum  $T$  such that a size  $N_t - 1$  family of  $T \times T$  Hurwitz-Radon matrices exists. It was shown in [3] that  $A(R, N_t)$  is finite for any  $R$ , and for full rate codes,

$$A(1, N_t) = \min_{0 \leq c, 0 \leq d < 4, 8c + 2^d \geq N_t} 2^{4c+d}.$$

Delay optimal real orthogonal codes (codes that achieve minimum  $T$ ) with full rate and full diversity are not square codes unless  $N_t = 2, 4$ , or  $8$ , but they do exist for all  $N_t$ . For example, we can construct codes for  $N_t = 7$  by deleting any column of an  $N_t = 8$  code.

For complex designs, a similar analysis shows that full rate and full diversity square orthogonal codes only exist for 2 transmit antennas. Given a complex orthogonal design of size  $N_t$ , Replace each symbol  $s_i = s_{i,r} + s_{i,q}j$  in the code matrix with

a  $2 \times 2$  matrix,

$$\begin{bmatrix} s_{i,r} & s_{i,q} \\ -s_{i,q} & s_{i,r} \end{bmatrix}.$$

The new code matrix formed is a real orthogonal design of size  $2N_t$ . Define  $A_c(R, N_t)$  to be the minimum  $T$  such that a  $T \times N_t$  complex orthogonal code matrix exists with at least rate  $R$ . For any  $R \leq 0.5$ ,  $A_c(R, N_t)$  is finite. In general for all  $R$ ,

$$A_c(R, N_t) \geq \frac{1}{2}A(R, 2N_t).$$

Delay optimal complex orthogonal codes with full rate and full diversity are not square codes unless  $N_t = 2$ , but they might exist for  $N_t > 2$ . Rate  $1/2$  codes are known to exist for all  $N_t$ , and only sporadic codes for  $R = 3/4$  are known for  $N_t = 3$  and  $N_t = 4$ .

Notice both real and complex orthogonal designs only consider linear codes designed to work for *all* possible symbol constellations. At this point, we define two classes of complex “non-linear” orthogonal codes:

- Class I designs: a  $T \times N_t$  matrix with linear or non-linear functions of  $s_i$  and  $s_i^*$ ,  $i = 1, \dots, L$ , as entries. The matrix must satisfy  $\mathbf{S}^H \mathbf{S} = \mathbf{D}_{N_t}$ , where  $\mathbf{D}_{N_t}$  is a diagonal matrix whose diagonal elements are linear combinations of the symbol energies.
- Class II designs: a  $T \times N_t$  matrix with linear combinations of  $s_i$  and  $s_i^*$ ,  $i = 1, \dots, L$ , as entries. The matrix must satisfy  $\mathbf{S}^H \mathbf{S} = \mathbf{D}_{N_t}$ , where  $\mathbf{D}_{N_t}$  is a diagonal matrix whose diagonal entries are linear or non-linear functions of the symbol energies.

These definitions do not guarantee full diversity or linear processing at the receiver, but allow more flexibility in designing codes. Note orthogonal codes are a special case

of non-linear orthogonal codes.

### E. Literature Review

Delay diversity [9], [10] and other related schemes [11], [12] were among the first techniques presented to exploit transmit diversity. Delay diversity can be viewed as a special case of space-time trellis coding (STTC), later developed by Tarokh et.al. [4]. The generalized approach combines trellis coded modulation (TCM) with transmit diversity techniques, and though decoding complexity for these codes grows exponentially with the number of antennas, they perform very well in slowly fading environments. The rank and determinant criteria emerged from this work and became a benchmark in space-time code design. A more structured method of STTC construction ensuring full diversity was later presented in [13].

The Alamouti code [14], remarkable for having an elegant and simple linear receiver, became a paradigm in space-time block coding (STBC). Alamouti's idea for two transmit antennas was generalized by orthogonal designs [3], [15], which have full diversity and linear maximum likelihood (ML) detectors that decouple the transmitted symbols. Unfortunately, the Hurwitz-Radon theorem showed that square complex linear processing orthogonal designs cannot achieve full diversity and full rate simultaneously, except in the two transmit antenna case [3], [16] (a formula for the maximum achievable data rate for square code matrices was given in [17]). For 3 or 4 transmit antennas, several orthogonal codes have been discovered with full diversity and a rate of  $3/4$  [3], [15]–[18]. As shown in [19], though, it is possible to design orthogonal, full rate and full diversity complex codes for more than two transmit antennas for *specific* signal constellations.

Similarly to orthogonal codes, unitary space-time modulation [20] and differential

unitary modulation [5] use a set of unitary code matrices to represent data. In general, the optimal receiver for a unitary modulation code is more complex than for an orthogonal design because the code matrix is not structured by symbols that can be decoupled for detection. These codes are typically non-square and designed for systems where channel state information (CSI) is unknown at the receiver.

The ABBA code presented in [21] and similar codes [22]–[24] have full rate, but are quasi-orthogonal<sup>3</sup> and offer a diversity order of only 2. The STTD-OTD code [25] provides some diversity gain by grouping symbols into Alamouti blocks and transforming them using a Walsh-Hadamard matrix. For the 4 transmit antenna case, this orthogonal code has full rate and diversity order 2. Recently, an orthogonal full diversity, full rate STBC for 4 transmit antennas was presented in [30]. However perfect knowledge of the channel at the transmitter and receiver is required to cancel inter-symbol-interference (ISI) and ensure orthogonality.

It has been shown that full diversity and full rate can be achieved with generalized algebraic space-time (GAST) codes, which use rotated constellations with a Hadamard transform [26]. In addition, these non-orthogonal codes offer a coding gain over comparable orthogonal codes, especially for large constellations and many transmit antennas. Another code in the literature utilizes space-time diversity with unitary constellation rotating precoders [27]–[29]. Constellation rotating codes essentially transmit a linear combination of the phase-rotated symbols through one antenna at a time, while leaving the other antennas silent. These codes are distinct for achieving full rate and full diversity, but are not orthogonal.

---

<sup>3</sup>Define  $\mathbf{Z}_i$  to be the  $i^{\text{th}}$  column of the code matrix  $\mathbf{S}$ ,  $i = 1, \dots, N_t$ . A code is quasi-orthogonal if the  $\mathbf{Z}_i$  can be divided into at least 2 sets such that the subspace formed by the span of all vectors within any set is orthogonal to the span of all other sets [22]. A measure of non-orthogonality was proposed in [21].

## CHAPTER II

## A CLASS I NON-LINEAR ORTHOGONAL CODE

In this chapter, we introduce a class I non-linear orthogonal code for 4 transmit antennas.<sup>1</sup> Instead of designing orthogonal block codes based on an assumption of linear receiver processing and full diversity, we only assume the code is rate 1. We then specify the most general form of a square class I non-linear orthogonal code and find convenient special cases with full rate. This design approach does not guarantee full diversity, so additional techniques are needed to improve diversity order.

Two examples of the new design approach are given in Section A and Section B, which result in the Alamouti code [14] and STTD-OTD code [25], respectively. The new code is given in Section C, followed by an analysis of linearity in Section D and diversity in Section E.

## A. An Example: The Alamouti Code

Consider designing a square space-time code utilizing two transmit antennas. The most general form of this space-time code is given by

$$\mathbf{S} = \begin{bmatrix} a_{11} & a_{12} \\ a_{21} & a_{22} \end{bmatrix}, \quad (2.1)$$

---

<sup>1</sup>See Section D of Chapter 1 for a definition of class I codes.

where the  $a_{ij}$  are complex symbols. Note  $\mathbf{S}^H \mathbf{S}$  has the following form.

$$\begin{aligned} \mathbf{S}^H \mathbf{S} &= \begin{bmatrix} a_{11}^* & a_{21}^* \\ a_{12}^* & a_{22}^* \end{bmatrix} \cdot \begin{bmatrix} a_{11} & a_{12} \\ a_{12} & a_{22} \end{bmatrix} \\ &= \begin{bmatrix} |a_{11}|^2 + |a_{21}|^2 & a_{11}^* a_{12} + a_{21}^* a_{22} \\ a_{12}^* a_{11} + a_{22}^* a_{21} & |a_{12}|^2 + |a_{22}|^2 \end{bmatrix}. \end{aligned} \quad (2.2)$$

The code is orthogonal only if  $\mathbf{S}^H \mathbf{S}$  is diagonal, i.e., when  $a_{11}^* a_{12} + a_{21}^* a_{22} = 0$ . Thus, the most general form of a 2 transmit antenna orthogonal code is in given by (2.1) with  $a_{22} = -a_{11}^* a_{12} / a_{21}^*$ , or

$$\mathbf{S} = \begin{bmatrix} a_{11} & a_{12} \\ a_{21} & -\frac{a_{11}^* a_{12}}{a_{21}^*} \end{bmatrix}. \quad (2.3)$$

Observe that this code matrix is a function of three symbol variables. By setting  $a_{21} = -a_{12}^*$  we obtain the well-known Alamouti code [14],

$$\mathbf{S} = \begin{bmatrix} a_{11} & a_{12} \\ -a_{12}^* & a_{11}^* \end{bmatrix}.$$

## B. An Example: STTD-OTD

We are now interested in the general form of a square orthogonal codes for 4 transmit antennas. Following the same procedure in the previous section, it can be shown that any  $4 \times 4$  orthogonal matrix has the form

$$\mathbf{S} = \begin{bmatrix} a_{11} & a_{12} & a_{13} & a_{14} \\ a_{21} & a_{22} & a_{23} & b_{24} \\ a_{31} & a_{32} & b_{33} & b_{34} \\ a_{41} & b_{42} & b_{43} & b_{44} \end{bmatrix}, \quad (2.4)$$

where

$$b_{42} = - (a_{41}^*)^{-1} \begin{bmatrix} a_{11}^* & a_{21}^* & a_{31}^* \end{bmatrix} \begin{bmatrix} a_{12} \\ a_{22} \\ a_{32} \end{bmatrix},$$

$$\begin{bmatrix} b_{33} \\ b_{43} \end{bmatrix} = - \left( \begin{bmatrix} a_{31} & a_{32} \\ a_{41} & a_{42} \end{bmatrix}^H \right)^{-1} \begin{bmatrix} a_{11}^* + a_{21}^* \\ a_{12}^* + a_{22}^* \end{bmatrix} \begin{bmatrix} a_{13} \\ a_{23} \end{bmatrix},$$

$$\begin{bmatrix} b_{24} \\ b_{34} \\ b_{44} \end{bmatrix} = - \left( \begin{bmatrix} a_{21} & a_{22} & a_{23} \\ a_{31} & a_{32} & a_{33} \\ a_{41} & a_{42} & a_{43} \end{bmatrix}^H \right)^{-1} \begin{bmatrix} a_{11}^* \\ a_{12}^* \\ a_{13}^* \end{bmatrix} a_{14}.$$

Symbols  $a_{ij}$  completely specify the space-time code. The elements  $b_{ij}$  in the lower right triangle portion of the data matrix are viewed as parity check elements, which force orthogonality. Define  $a_{11} = s_1$ ,  $a_{12} = s_2$ ,  $a_{13} = s_3$ ,  $a_{14} = s_4$ ,  $a_{21} = -s_2^*$ ,  $a_{22} = s_1^*$ ,  $a_{23} = -s_4^*$ ,  $a_{31} = s_1$ ,  $a_{32} = s_2$ , and  $a_{41} = -s_2^*$ . Then (2.4) simplifies to

$$\mathbf{S} = \begin{bmatrix} s_1 & s_2 & s_3 & s_4 \\ -s_2^* & s_1^* & -s_4^* & s_3^* \\ s_1 & s_2 & -s_3 & -s_4 \\ -s_2^* & s_1^* & s_4^* & -s_3^* \end{bmatrix}, \quad (2.5)$$

which is the STTD-OTD code [25]. Notice we have created an orthogonal code using this new design approach.

### C. The New Code Matrix

In (2.4), define  $a_{11} = s_1$ ,  $a_{12} = s_2$ ,  $a_{13} = s_3$ ,  $a_{14} = s_4$ ,  $a_{21} = -s_2^*$ ,  $a_{22} = s_1^*$ ,  $a_{23} = -s_4^*$ ,  $a_{31} = s_3$ ,  $a_{32} = s_4$ , and  $a_{41} = -s_4^*$ . After simplifying, the code matrix reduces to

$$\mathbf{S} = \begin{bmatrix} s_1 & s_2 & s_3 & s_4 \\ -s_2^* & s_1^* & -s_4^* & s_3^* \\ s_3 & s_4 & x & y \\ -s_4^* & s_3^* & -y^* & x^* \end{bmatrix}, \quad (2.6)$$

where

$$x = s_1 - ls_3,$$

$$y = s_2 - ls_4,$$

$$l = \frac{\Re(s_1s_3^* + s_2s_4^*)}{E} = \cos(\angle s_1 - \angle s_3) + \cos(\angle s_2 - \angle s_4).$$

The data matrix (2.6) can be expressed as

$$\begin{aligned} \mathbf{S} &= \begin{bmatrix} s_1 & s_2 & s_3 & s_4 \\ -s_2^* & s_1^* & -s_4^* & s_3^* \\ s_3 & s_4 & s_1 & s_2 \\ -s_4^* & s_3^* & -s_2^* & s_1^* \end{bmatrix} - l \begin{bmatrix} 0 & 0 & 0 & 0 \\ 0 & 0 & 0 & 0 \\ 0 & 0 & s_3 & s_4 \\ 0 & 0 & -s_4^* & s_3^* \end{bmatrix} \\ &= \begin{bmatrix} \mathbf{A} & \mathbf{B} \\ \mathbf{B} & \mathbf{A} - l\mathbf{B} \end{bmatrix}, \end{aligned} \quad (2.7)$$

where  $\mathbf{A}$  and  $\mathbf{B}$  are Alamouti blocks. Notice the new code resembles the ABBA code [21] with a new parameter  $l$ , which ensures orthogonality.

#### D. Linearity

It is easy to verify that

$$\mathbf{S}^H \mathbf{S} = \left( \sum_{i=1}^4 |s_i|^2 \right) \mathbf{I}_4. \quad (2.8)$$

However the optimal receiver for the new code is generally non-linear and cannot decouple symbols because the code matrix itself is non-linear. This property is characteristic of class I non-linear orthogonal codes. However, the new code will be linear for symbol constellations where  $l$  is constant. In particular, if  $l = 0$ ,

$$\mathbf{S} = \begin{bmatrix} \mathbf{A} & \mathbf{B} \\ \mathbf{B} & \mathbf{A} \end{bmatrix}. \quad (2.9)$$

This is the ABBA code [21], which is not orthogonal in general, but we show it is orthogonal for constellations where  $l = 0$ .

Notice when symbols  $s_1$  and  $s_2$  are real and  $s_3$  and  $s_4$  are imaginary,  $l = 0$ . Thus, for rotated PAM constellations where symbols  $s_3$  and  $s_4$  are rotated by  $\pi/2$  with respect to  $s_1$  and  $s_2$ , the new code is linear.

#### E. Diversity Analysis

If the symbols have the binary constellations,

$$\begin{aligned} s_1, s_2 &\in \pm 1, \\ s_3, s_4 &\in \pm j, \end{aligned}$$

the code achieves full diversity. In addition, the code is also full rate and linear ( $l = 0$ ). Thus, the new code is a complex square orthogonal code with full rate and diversity for 4 transmit antennas when using this *specific* rotated BPSK constellation.

Now consider the new code with ordinary QPSK constellations. From perfor-

mance plots, it is clear the new code does not have full diversity. One technique to increase diversity at the expense of data rate is to use a finite state machine (FSM) to avoid symbol combinations which degrade the diversity of the code.

Before designing a FSM, we first study the code matrix to understand why it does not achieve full diversity. The new code with QPSK symbols has

- 256 data matrices.
- $\binom{256}{2} = 256 \cdot 255/2 = 32640$  unique data matrix pairs.
- 384 “failing” matrix pairs (which cause the diversity product to be zero).

The failing matrix pairs are pairs of code matrices  $\mathbf{S}$  and  $\tilde{\mathbf{S}}$  such that  $\det(\mathbf{S} - \tilde{\mathbf{S}}) = 0$ . We discovered all failing matrix pairs contained at least one code matrix from a small set of “bad” matrices that must be avoided to achieve full diversity. Before eliminating all bad matrices with a FSM, constellation phase rotations are used to reduce the number of bad matrices and optimize data rate. By empirically testing some phase rotations, it is quickly clear that the number of failing matrix pairs and bad code matrices can indeed be reduced. Example data is included in Appendix A.

Quite unexpectedly, it was seen that the rotation  $[\phi_1, \phi_2, \phi_3, \phi_4] = [0, 1, 3, 5] \pi/8$ , where  $\phi_i$  is the counter-clockwise rotation of symbol  $s_i$ , has no failing matrix pairs ( $\zeta_v = 0.0058$ ). Thus, full diversity is achieved and a FSM is not needed to improve the diversity order of the code. With an exhaustive search of all phase shifts in increments of  $\pi/4096$ , the best phase set found was  $[0, 0, 32, 19] \pi/128$  ( $\zeta_v = 0.403775$ ).

There are two key points about this new code. First, with BPSK based constellations it shows that linear complex square orthogonal codes with full rate and full diversity can exist for *specific* constellations. Second, we have seen that rotating symbol constellations is a useful tool to improve diversity.

## CHAPTER III

## A CLASS II NON-LINEAR ORTHOGONAL CODE

In this chapter, we introduce a new class II non-linear orthogonal code.<sup>1</sup> The following heuristic method is used to find the subsequent code. We start with a linear orthogonal space-time code with less than full diversity utilizing the appropriate number of transmit antennas and time intervals per block. To guarantee each symbol is seen through each channel, the transmitted symbols of the code matrix are encoded with linear combinations of “base” data symbols. For a fair comparison of performance, the modification must maintain the same average transmit power. The diversity product (1.2) is used as a test to search for symbol constellations that allow the modified code to achieve full diversity. PAM and PSK based constellations are considered.

The new code is developed in Section A. Analysis of code linearity and diversity are covered in Sections B and C, respectively. In Section D, specific constellations are designed for the code. It is shown that for PAM based constellations, the code is a square, full rate, full diversity complex orthogonal design for 4 transmit antennas. Capacity is discussed in Section E. Finally, in Sections F and G, receivers for when fading is known and when fading is unknown are outlined, respectively. For known fading, the optimal receiver decouples the symbol detection problem into pairs. With PAM based constellations where the code is orthogonal, this receiver simplifies to complete symbol decoupling.

---

<sup>1</sup>See Section D of Chapter 1 for a definition of class II codes.

### A. The New Code Matrix

Our goal is to design a square, full rate, full diversity, 4 transmit antenna space-time block code with  $M$ -ary constellations. We start with the orthogonal STTD-OTD code [25] defined as,

$$\mathbf{S} = \begin{bmatrix} s_1 & s_2 & s_3 & s_4 \\ -s_2^* & s_1^* & -s_4^* & s_3^* \\ s_1 & s_2 & -s_3 & -s_4 \\ -s_2^* & s_1^* & s_4^* & -s_3^* \end{bmatrix} = \begin{bmatrix} \mathbf{A} & \mathbf{B} \\ \mathbf{A} & -\mathbf{B} \end{bmatrix}, \quad (3.1)$$

where  $\mathbf{A}$  and  $\mathbf{B}$  are Alamouti blocks. This code alone has a diversity order of 2, which is easily seen since each symbol is transmitted through only 2 of the 4 transmit antennas. Since each symbol must be transmitted over every antenna to achieve full diversity, it is clear that a modification of the code matrix is required. We encode the transmitted symbols as follows.

$$s_1 = \frac{d_1 + d_2}{\sqrt{2}}, \quad (3.2)$$

$$s_2 = \frac{d_3 + d_4}{\sqrt{2}}, \quad (3.3)$$

$$s_3 = \frac{d_1 - d_2}{\sqrt{2}}, \quad (3.4)$$

$$s_4 = \frac{d_3 - d_4}{\sqrt{2}}, \quad (3.5)$$

where  $d_1$ ,  $d_2$ ,  $d_3$ , and  $d_4$  are complex “base” symbols representing the data and  $s_1$ ,  $s_2$ ,  $s_3$ , and  $s_4$  are complex transmitted symbols. The  $\sqrt{2}$  is necessary to normalize

energy.<sup>2</sup> Note the transformation (3.2)–(3.5) can be written as

$$\begin{bmatrix} s_1 \\ s_2 \\ s_3 \\ s_4 \end{bmatrix} = \frac{1}{\sqrt{2}} \begin{bmatrix} 1 & 1 & 0 & 0 \\ 0 & 0 & 1 & 1 \\ 1 & -1 & 0 & 0 \\ 0 & 0 & 1 & -1 \end{bmatrix} \begin{bmatrix} d_1 \\ d_2 \\ d_3 \\ d_4 \end{bmatrix}, \quad (3.6)$$

or

$$\begin{bmatrix} s_1 \\ s_3 \end{bmatrix} = \frac{1}{\sqrt{2}} \begin{bmatrix} 1 & 1 \\ 1 & -1 \end{bmatrix} \begin{bmatrix} d_1 \\ d_2 \end{bmatrix}, \quad \begin{bmatrix} s_2 \\ s_4 \end{bmatrix} = \frac{1}{\sqrt{2}} \begin{bmatrix} 1 & 1 \\ 1 & -1 \end{bmatrix} \begin{bmatrix} d_3 \\ d_4 \end{bmatrix}. \quad (3.7)$$

With this transformation, the new data matrix can be expressed as

$$\begin{aligned} \mathbf{S} &= \frac{1}{\sqrt{2}} \begin{bmatrix} d_1 + d_2 & d_3 + d_4 & d_1 - d_2 & d_3 - d_4 \\ -d_3^* - d_4^* & d_1^* + d_2^* & -d_3^* + d_4^* & d_1^* - d_2^* \\ d_1 + d_2 & d_3 + d_4 & -d_1 + d_2 & -d_3 + d_4 \\ -d_3^* - d_4^* & d_1^* + d_2^* & d_3^* - d_4^* & -d_1^* + d_2^* \end{bmatrix} \\ &= \frac{1}{\sqrt{2}} \begin{bmatrix} d_1 & d_3 & d_1 & d_3 \\ -d_3^* & d_1^* & -d_3^* & d_1^* \\ d_1 & d_3 & -d_1 & -d_3 \\ -d_3^* & d_1^* & d_3^* & -d_1^* \end{bmatrix} + \frac{1}{\sqrt{2}} \begin{bmatrix} d_2 & d_4 & -d_2 & -d_4 \\ -d_4^* & d_2^* & d_4^* & -d_2^* \\ d_2 & d_4 & d_2 & d_4 \\ -d_4^* & d_2^* & -d_4^* & d_2^* \end{bmatrix} \\ &= \frac{1}{\sqrt{2}} \begin{bmatrix} \mathbf{C} & \mathbf{C} \\ \mathbf{C} & -\mathbf{C} \end{bmatrix} + \frac{1}{\sqrt{2}} \begin{bmatrix} \mathbf{D} & -\mathbf{D} \\ \mathbf{D} & \mathbf{D} \end{bmatrix}, \quad (3.8) \end{aligned}$$

where  $\mathbf{C}$  and  $\mathbf{D}$  are Alamouti blocks.

---

<sup>2</sup>We assume the constellations of  $d_i$ ,  $i = 1, \dots, 4$ , are centered about the origin of the complex plane and that each constellation point is equally likely, so  $\mathbb{E}[d_i] = 0$ . Then the normalization in (3.2)–(3.5) is valid and the average energies of symbols  $d_i$  are the same as the average energies of symbols  $s_i$ . For example,  $\mathbb{E}[s_1 s_1^*] = \frac{1}{2} \mathbb{E}[d_1 d_1^*] + \frac{1}{2} \mathbb{E}[d_2 d_2^*] + \frac{1}{2} \mathbb{E}[d_1] \mathbb{E}[d_2^*] + \frac{1}{2} \mathbb{E}[d_2] \mathbb{E}[d_1^*] = \mathbb{E}[d_i d_i^*] = E$ .

## B. Linearity

When using a linear transformation like (3.2)–(3.5) on the symbols of a sub-full diversity orthogonal space-time code, the receiver will become non-linear for most constellations by introducing quadratic terms into  $\mathbf{S}^H \mathbf{S}$ . In this case,  $\mathbf{S}^H \mathbf{S}$  for the new code is non-linear as shown below.

$$\begin{aligned}
\mathbf{S}^H \mathbf{S} &= \begin{bmatrix} |s_1|^2 + |s_2|^2 & 0 & 0 & 0 \\ 0 & |s_1|^2 + |s_2|^2 & 0 & 0 \\ 0 & 0 & |s_3|^2 + |s_4|^2 & 0 \\ 0 & 0 & 0 & |s_3|^2 + |s_4|^2 \end{bmatrix} \\
&= \begin{bmatrix} (|d_1 + d_2|^2 + |d_3 + d_4|^2) \mathbf{I}_2 & \mathbf{0}_2 \\ \mathbf{0}_2 & (|d_1 - d_2|^2 + |d_3 - d_4|^2) \mathbf{I}_2 \end{bmatrix} \\
&= \begin{bmatrix} (\sum_{i=1}^4 |d_i|^2 + k) \mathbf{I}_2 & \mathbf{0}_2 \\ \mathbf{0}_2 & (\sum_{i=1}^4 |d_i|^2 - k) \mathbf{I}_2 \end{bmatrix} \\
&= \left( \sum_{i=1}^4 |d_i|^2 \right) \mathbf{I}_4 + k \begin{bmatrix} \mathbf{I}_2 & \mathbf{0}_2 \\ \mathbf{0}_2 & -\mathbf{I}_2 \end{bmatrix}, \tag{3.9}
\end{aligned}$$

where

$$k = 2\Re(d_1 d_2^* + d_3 d_4^*). \tag{3.10}$$

The code is orthogonal in the sense that  $\mathbf{S}^H \mathbf{S}$  is diagonal, but the non-linear term  $k$  causes the code to appear quasi-orthogonal in terms of receiver complexity. Thus, the new code is a class II non-linear orthogonal code.

### C. Diversity Analysis

Note the following property of determinants:

$$\det \left( \begin{bmatrix} \mathbf{A} & \mathbf{B} \\ \mathbf{C} & \mathbf{D} \end{bmatrix} \right) = \det(\mathbf{A}) \det(\mathbf{D} - \mathbf{C}\mathbf{A}^{-1}\mathbf{B}). \quad (3.11)$$

To compute the diversity product (1.2) for the new code, (3.11) is used to evaluate  $\det(\mathbf{S} - \tilde{\mathbf{S}})$  as shown below.

$$\begin{aligned} \det(\mathbf{S} - \tilde{\mathbf{S}}) &= \det \left( \begin{bmatrix} \mathbf{A} & \mathbf{B} \\ \mathbf{A} & -\mathbf{B} \end{bmatrix} - \begin{bmatrix} \tilde{\mathbf{A}} & \tilde{\mathbf{B}} \\ \tilde{\mathbf{A}} & -\tilde{\mathbf{B}} \end{bmatrix} \right) \\ &= \det(\mathbf{A} - \tilde{\mathbf{A}}) \det \left( -\mathbf{B} + \tilde{\mathbf{B}} - (\mathbf{A} - \tilde{\mathbf{A}}) (\mathbf{A} - \tilde{\mathbf{A}})^{-1} (\mathbf{B} - \tilde{\mathbf{B}}) \right) \\ &= 4 \det(\mathbf{A} - \tilde{\mathbf{A}}) \det(\mathbf{B} - \tilde{\mathbf{B}}), \end{aligned} \quad (3.12)$$

where  $\mathbf{S}$  and  $\tilde{\mathbf{S}}$  are matrices of the form (3.1) and  $\mathbf{A}$ ,  $\tilde{\mathbf{A}}$ ,  $\mathbf{B}$ , and  $\tilde{\mathbf{B}}$  are Alamouti blocks defined accordingly. Furthermore, notice

$$\begin{aligned} \det(\mathbf{A} - \tilde{\mathbf{A}}) &= \det \left( \begin{bmatrix} s_1 & s_2 \\ -s_2^* & s_1^* \end{bmatrix} - \begin{bmatrix} \tilde{s}_1 & \tilde{s}_2 \\ -\tilde{s}_2^* & \tilde{s}_1^* \end{bmatrix} \right) \\ &= |s_1 - \tilde{s}_1|^2 + |s_2 - \tilde{s}_2|^2 \\ &= \frac{1}{2} \left[ |d_1 + d_2 - \tilde{d}_1 - \tilde{d}_2|^2 + |d_3 + d_4 - \tilde{d}_3 - \tilde{d}_4|^2 \right], \end{aligned} \quad (3.13)$$

where  $s_1$  and  $s_2$  are symbols in Alamouti block  $\mathbf{A}$  and definitions for base symbols  $d_1$  through  $d_4$  follow from (3.2)–(3.5). For full diversity we require  $\det(\mathbf{A} - \tilde{\mathbf{A}}) \neq 0$  whenever any symbol in  $\mathbf{S}$  differs from the corresponding symbol in  $\tilde{\mathbf{S}}$ . Thus,

$$d_1 - \tilde{d}_1 + d_2 - \tilde{d}_2 \neq 0, \quad (3.14)$$

$$d_3 - \tilde{d}_3 + d_4 - \tilde{d}_4 \neq 0, \quad (3.15)$$

where (3.14) must hold when  $d_1 \neq \tilde{d}_1$  or  $d_2 \neq \tilde{d}_2$ , and (3.15) must hold when  $d_3 \neq \tilde{d}_3$  or  $d_4 \neq \tilde{d}_4$ . A similar result follows from  $\det(\mathbf{B} - \tilde{\mathbf{B}})$ .

To design constellations for the new code, first consider (3.14). Note  $d_i - \tilde{d}_i$  has a finite number of possible values because  $d_i$  is drawn from a finite size constellation. As long as the constellation for  $-d_2 + \tilde{d}_2$  does not contain points that overlap with the unrotated  $d_1 - \tilde{d}_1$  constellation (except at the origin where  $d_i = \tilde{d}_i$ ), equation (3.14) holds. Using similar reasoning, we use (3.15) to design constellations for  $d_3$  and  $d_4$ . Consider constellations that satisfy (3.14) and (3.15) using symbol phase rotations. For example, suppose each base symbol has identical constellations, except symbols  $d_2$  and  $d_4$  are rotated by an angle  $\phi$  with respect to  $d_1$  and  $d_3$ . Then the constellations for  $d_2 - \tilde{d}_2$  and  $d_4 - \tilde{d}_4$  are also rotated by  $\phi$  with respect to  $d_1 - \tilde{d}_1$  and  $d_3 - \tilde{d}_3$ . Since there are only a discrete number of points in each  $d_i - \tilde{d}_i$  constellation and an infinite range of phase rotations, clearly there are infinitely many phase shifts,  $\phi$ , that offer full diversity.

## D. Constellation Design

### 1. PAM Based Constellations

Note from (3.9) that any set of symbol constellations such that  $k = 0$  results in a linear orthogonal code with full diversity, since the coefficients of the energy terms in  $\mathbf{S}^H \mathbf{S}$  are strictly positive. Similarly to the class I non-linear code in the previous chapter, by restricting base symbols  $d_1$  and  $d_3$  to be real and  $d_2$  and  $d_4$  to be imaginary,  $k = 0$  and  $\mathbf{S}^H \mathbf{S} = (|d_1|^2 + |d_2|^2 + |d_3|^2 + |d_4|^2) \mathbf{I}_4$ . Thus, when the base symbols are drawn from PAM constellations as shown in Fig. 3(a), where symbols  $d_2$  and  $d_4$  are rotated by  $\pi/2$  with respect to real symbols  $d_1$  and  $d_3$ , the code is a square complex orthogonal design with full diversity. In this case, each transmitted symbol,

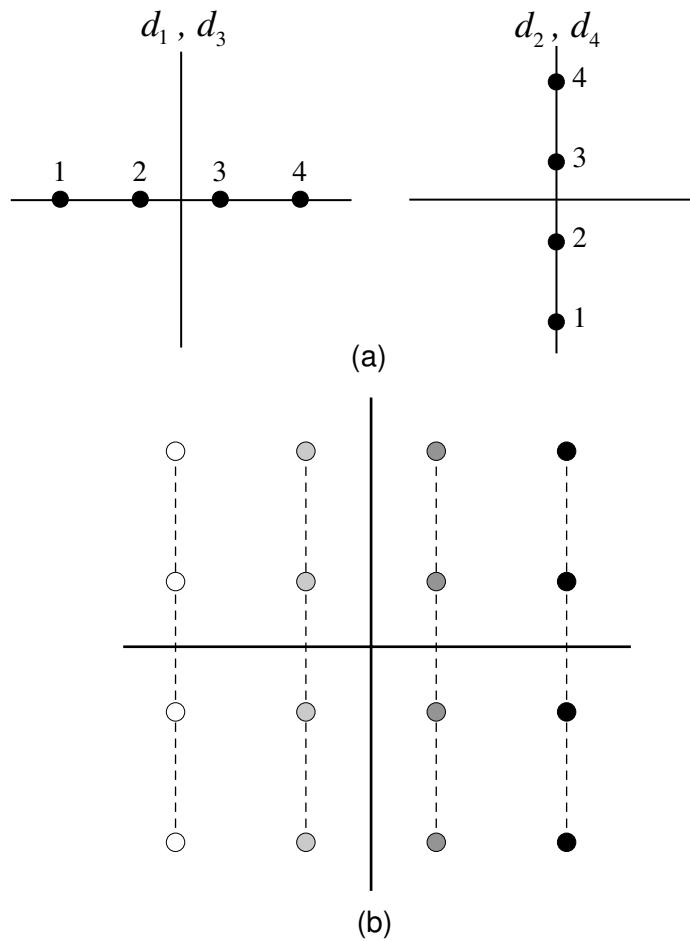


Fig. 3. (a) Constellations for PAM base symbols; (b) Resulting QAM transmit constellation.

$s_i$ ,  $i = 1, \dots, 4$ , is drawn from a QAM constellation as shown in Fig. 3(b). In the illustration, constellation points are grouped by color. All points of a single color represent the constellation of  $d_2$  (or  $d_4$ , depending on which  $s_i$  we consider). Each group is centered on a constellation point in  $d_1$  (or  $d_3$ ).

## 2. PSK Based Constellations

Consider uniform  $M$ -PSK base constellations with  $d_2$  and  $d_4$  rotated by  $\pi/M$  with respect to  $d_1$  and  $d_3$ . In this case, (3.14) and (3.15) are satisfied and the code will

achieve full diversity. QPSK base symbol constellations with  $d_2$  and  $d_4$  rotated by  $\pi/4$  with respect to  $d_1$  and  $d_3$  are shown in Fig. 4(a). Each transmitted symbol,  $s_i$ , has 16 possible values depending on the QPSK base symbols,  $d_i$ , as depicted in Fig. 4(b). In the illustration, 4 groups of 4 constellation points are shown with each group having a different shade of gray. These groups represent the constellation of  $d_2$  (or  $d_4$ ). The center of each group represents the constellation of  $d_1$  (or  $d_3$ ). Notice the phase rotation  $\pi/4$  maximizes minimum transmitted symbol distance.

One fear in using constellation rotations in practice is a high sensitivity to phase error. However, this code is relatively robust in the sense that the diversity product is not vulnerable to a small phase shift error between even ( $d_2$  and  $d_4$ ) and odd ( $d_1$  and  $d_3$ ) base symbol constellations. This is illustrated in Fig. 5 with a plot of the diversity product for QPSK symbols. The diversity product is near its maximum value for a wide range of phases centered about  $\pi/4$ , and is only zero when no phase shift is used.

### E. Capacity

Ignoring the restriction in symbol constellations, we compute the capacity of a MIMO channel using the new code in (3.8). To compute capacity for one receive antenna, note equation (1.1) can be converted to the following form,

$$\tilde{\mathbf{R}} = \mathbf{X} \cdot \tilde{\mathbf{H}} + \tilde{\mathbf{N}}, \quad (3.16)$$

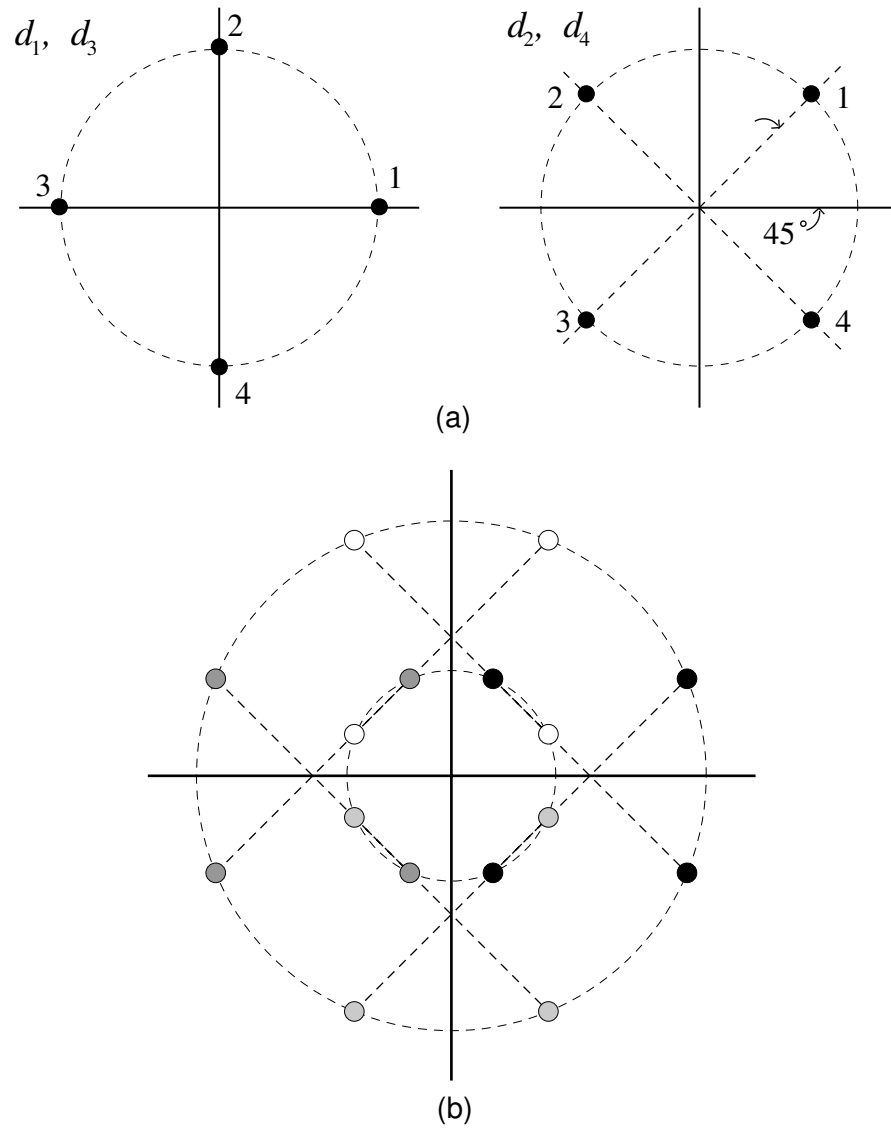


Fig. 4. (a) Constellations for QPSK base symbols; (b) Resulting transmit constellation.

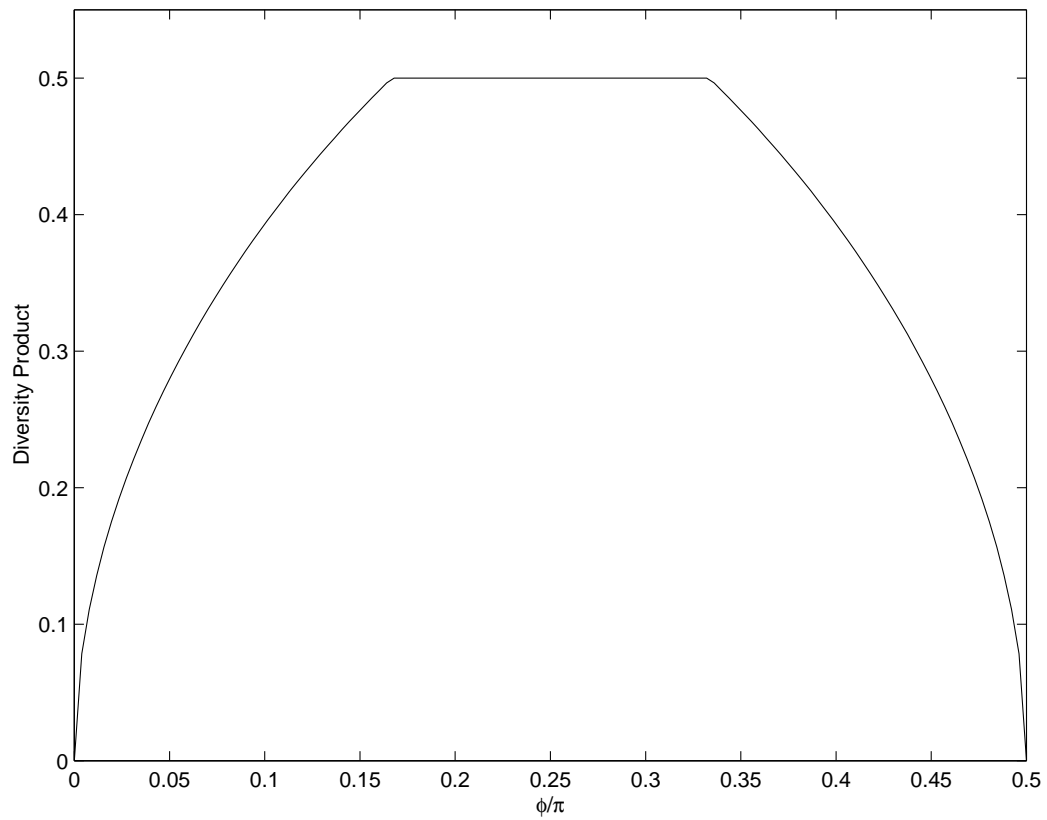


Fig. 5. Diversity product of the class II non-linear code with QPSK base symbols;  $d_2$  and  $d_4$  are rotated by  $\phi$  with respect to  $d_1$  and  $d_3$ .

where

$$\begin{aligned}
\tilde{\mathbf{R}} &= \begin{bmatrix} r_1 & r_2^* & r_3 & r_4^* \end{bmatrix}, \\
\tilde{\mathbf{N}} &= \begin{bmatrix} n_1 & n_2^* & n_3 & n_4^* \end{bmatrix}, \\
\mathbf{X} &= \begin{bmatrix} d_1 & d_2 & d_3 & d_4 \end{bmatrix}, \\
\tilde{\mathbf{H}} &= \frac{1}{\sqrt{2}} \begin{bmatrix} h_1 + h_3 & h_2^* + h_4^* & h_1 - h_3 & h_2^* - h_4^* \\ h_1 - h_3 & h_2^* - h_4^* & h_1 + h_3 & h_2^* + h_4^* \\ h_2 + h_4 & -h_1^* - h_3^* & h_2 - h_4 & -h_1^* + h_3^* \\ h_2 - h_4 & -h_1^* + h_3^* & h_2 + h_4 & -h_1^* - h_3^* \end{bmatrix}, \tag{3.17}
\end{aligned}$$

and  $r_i$  represents the received statistic at time  $i$ ,  $n_i$  is the AWGN in  $r_i$ ,  $h_j$  represents the channel fading between antenna  $j$  and the receive antenna, and  $d_i$  are the base symbols of the code. In this form, it is clear that the capacity of the new code is identical to a MIMO channel whose fading matrix is given by  $\tilde{\mathbf{H}}$ .

Plots of code capacity and optimal capacity for a MIMO channel (1.3) are shown in Fig. 6 for one receive antenna. The expectations were computed using Monte-Carlo simulations. Note that capacity of the new code is identical to STTD-OTD and lies about 2 dB from MIMO capacity.

## F. Receivers for Known Fading

### 1. Optimal Receivers

When fading is known, the optimal receiver decision rule for a space-time block code is given by

$$\max_{\mathbf{S}} \Re \left[ \text{trace} \left( 2\mathbf{R}^H \mathbf{S} \mathbf{H} - \mathbf{H}^H \mathbf{S}^H \mathbf{S} \mathbf{H} \right) \right]. \tag{3.18}$$

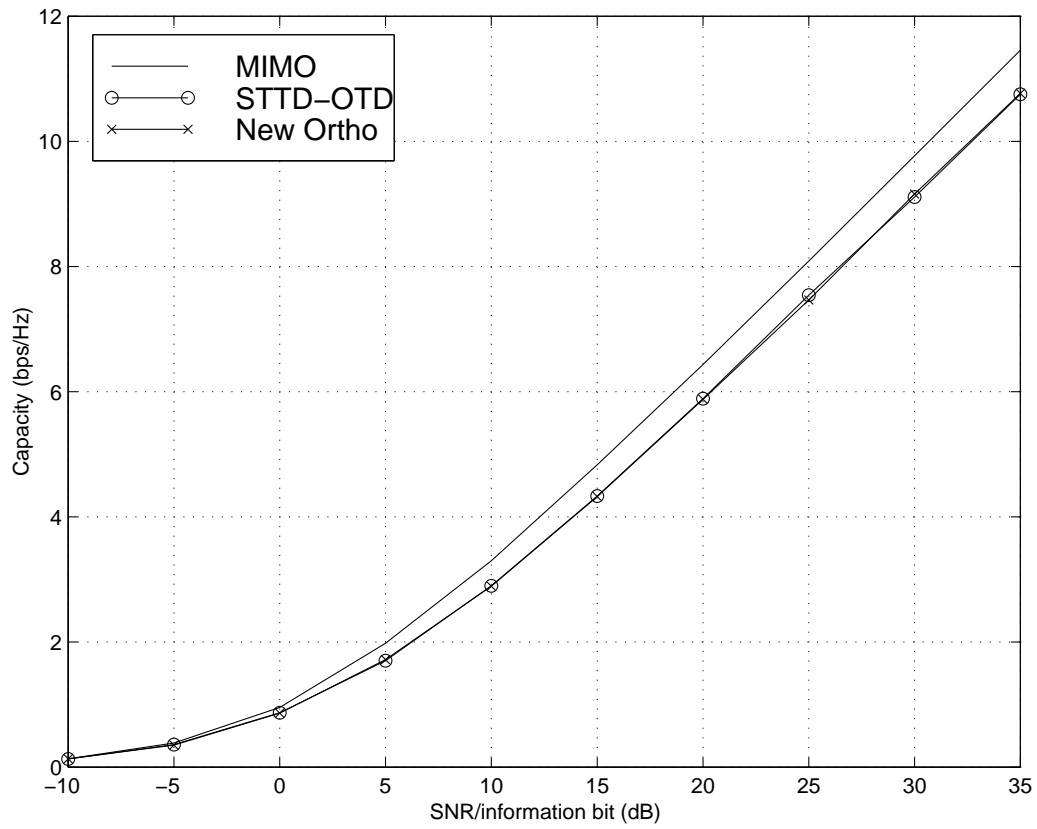


Fig. 6. Capacity of the class II non-linear orthogonal code.

With one receive antenna, the decision further simplifies to

$$\max_{\mathbf{S}} 2\Re(\mathbf{R}^H \mathbf{S} \mathbf{H}) - \mathbf{H}^H \mathbf{S}^H \mathbf{S} \mathbf{H}. \quad (3.19)$$

For simplicity, assume  $N_r = 1$ . In general, the decision rule for the new code with complex base symbols (e.g., PSK or QAM) follows from (3.19). After simplifying, the decision rule in terms of  $s_i$  is

$$\max_{s_1, s_3} \Re(y_1^* s_1 + y_3^* s_3) - \widetilde{F}_1 |s_1|^2 - \widetilde{F}_3 |s_3|^2, \quad (3.20)$$

$$\max_{s_2, s_4} \Re(y_2^* s_2 + y_4^* s_4) - \widetilde{F}_2 |s_2|^2 - \widetilde{F}_4 |s_4|^2, \quad (3.21)$$

where the received statistic at time  $i$  is denoted  $r_i$ , the fading over channel  $j$  is  $h_j$ , and

$$y_1 = x_1 h_1^* + x_2^* h_2,$$

$$y_2 = x_1 h_2^* - x_2^* h_1,$$

$$y_3 = x_3 h_3^* + x_4^* h_4,$$

$$y_4 = x_3 h_4^* - x_4^* h_3,$$

$$x_1 = r_1 + r_3,$$

$$x_2 = r_2 + r_4,$$

$$x_3 = r_1 - r_3,$$

$$x_4 = r_2 - r_4,$$

$$\widetilde{F}_1 = \widetilde{F}_2 = |h_1|^2 + |h_2|^2,$$

$$\widetilde{F}_3 = \widetilde{F}_4 = |h_3|^2 + |h_4|^2.$$

We cannot decouple  $s_1$  and  $s_3$  from  $s_2$  and  $s_4$  because of their dependence on  $d_i$ . In

terms of  $d_i$ , the optimal receiver is,

$$\max_{d_1, d_2} \Re(\tilde{r}_1^* d_1 + \tilde{r}_2^* d_2 - 2z d_1 d_2^*) - \tilde{E} |d_1|^2 - \tilde{E} |d_2|^2, \quad (3.22)$$

$$\max_{d_3, d_4} \Re(\tilde{r}_3^* d_3 + \tilde{r}_4^* d_4 - 2z d_3 d_4^*) - \tilde{E} |d_3|^2 - \tilde{E} |d_4|^2, \quad (3.23)$$

where

$$\tilde{r}_1 = y_1 + y_3,$$

$$\tilde{r}_2 = y_1 - y_3,$$

$$\tilde{r}_3 = y_2 + y_4,$$

$$\tilde{r}_4 = y_2 - y_4,$$

$$z = \frac{1}{\sqrt{2}} (|h_1|^2 + |h_2|^2 - |h_3|^2 - |h_4|^2),$$

$$\tilde{E} = \frac{1}{\sqrt{2}} \sum_{j=1}^{N_t} |h_j|^2.$$

This verifies that the receiver for the new code is generally not linear because  $\mathbf{S}^H \mathbf{S}$  is non-linear. However, the optimal receiver can at least decouple the base symbols into pairs. This results in significantly reduced receiver complexity.

#### a. Using PAM Base Constellations

For an orthogonal code with symbols  $d_i$  and  $\mathbf{S}^H \mathbf{S} = \sum_{i=1}^T |d_i|^2 \mathbf{I}_{N_t}$ , the optimal receiver is linear (with an energy term) and decouples the data symbols. i.e.,

$$\hat{d}_i = \arg \max_{d_i} \Re(d_i \tilde{r}_i^*) - \tilde{E}_i |d_i|^2, \quad i = 1, \dots, 4, \quad (3.24)$$

where  $\tilde{r}_i$  is a complex constant and  $\tilde{E}_i$  is a real constant.

The detector for our new code using the modified PAM base symbols reduces to the form (3.24) with  $\tilde{r}_i$  defined above and  $\tilde{E}_i = \tilde{E} \forall i$ . This simplification results

because the non-linear terms in (3.22) and (3.23) disappear.

b. Using PSK Base Constellations

For any PSK symbols, the optimal receiver in (3.22) and (3.23) can be simplified.

Since each symbol has equal energy, we have

$$\max_{d_1, d_2} \Re(\tilde{r}_1^* d_1 + \tilde{r}_2^* d_2 - 2z d_1 d_2^*), \quad (3.25)$$

$$\max_{d_3, d_4} \Re(\tilde{r}_3^* d_3 + \tilde{r}_4^* d_4 - 2z d_3 d_4^*). \quad (3.26)$$

## 2. Sub-Optimal Receivers

A sub-optimal receiver can be derived from (3.20) and (3.21) by decoupling symbols  $s_i$ , which results in the detection rule (3.24) with  $\tilde{r}_i = y_i$  and  $\widetilde{E}_i = \widetilde{F}_i$ . We compute a soft estimate of  $s_i$  using

$$\hat{s}_i = \frac{y_i}{2\widetilde{F}_i}. \quad (3.27)$$

From equations (3.2)–(3.5), sub-optimal estimates of base symbols  $d_i$  are generated by choosing symbols in the constellations of  $d_i$  closest to the following statistics.

$$\hat{d}_1 = \frac{1}{2\sqrt{2}} \left( \frac{y_1}{\widetilde{F}_1} + \frac{y_3}{\widetilde{F}_3} \right), \quad (3.28)$$

$$\hat{d}_2 = \frac{1}{2\sqrt{2}} \left( \frac{y_1}{\widetilde{F}_1} - \frac{y_3}{\widetilde{F}_3} \right), \quad (3.29)$$

$$\hat{d}_3 = \frac{1}{2\sqrt{2}} \left( \frac{y_2}{\widetilde{F}_2} + \frac{y_4}{\widetilde{F}_4} \right), \quad (3.30)$$

$$\hat{d}_4 = \frac{1}{2\sqrt{2}} \left( \frac{y_2}{\widetilde{F}_2} - \frac{y_4}{\widetilde{F}_4} \right). \quad (3.31)$$

Sub-optimal zero-forcing (ZF) and linear minimum mean square error (MMSE) receivers may also be used for simple linear receiver processing. A linear receiver

implements,

$$\hat{\mathbf{X}} = \tilde{\mathbf{R}}\mathbf{F}, \quad (3.32)$$

where  $\mathbf{X}$  and  $\tilde{\mathbf{R}}$  are defined in Section E. A ZF receiver uses

$$\mathbf{F} = \tilde{\mathbf{H}}^H \left( \tilde{\mathbf{H}}\tilde{\mathbf{H}}^H \right)^{-1}, \quad (3.33)$$

where  $\tilde{\mathbf{H}}$  is defined in (3.17). A linear MMSE receiver uses

$$\mathbf{F} = \tilde{\mathbf{H}}^H \left( \tilde{\mathbf{H}}\tilde{\mathbf{H}}^H + \frac{1}{\rho}\mathbf{I}_T \right)^{-1}. \quad (3.34)$$

The sub-optimal receiver in (3.28)–(3.31) is equivalent to the linear ZF receiver.

#### G. Receivers for Unknown Known Fading

The optimal receiver for a space-time block code with unknown fading has the decision rule

$$\min_{\mathbf{S}} \text{trace} \left( \mathbf{R}^H \mathbf{\Gamma}^{-1} \mathbf{R} \right) + \ln \det \mathbf{\Gamma},$$

where

$$\mathbf{\Gamma} = \mathbf{S}\mathbf{S}^H + \frac{1}{\rho}\mathbf{I}_T,$$

and  $\rho$  is SNR (we assume symbols in  $\mathbf{S}$  have unit average energy). If we further assume a linear orthogonal code with equal energy symbols, then the term  $\det \mathbf{\Gamma}$  is not a function of the data. For one receive antenna, the detector reduces to

$$\max_{\mathbf{S}} \mathbf{R}^H \mathbf{S}\mathbf{S}^H \mathbf{R}.$$

To estimate the channel, we insert pilot symbols into the data frame and assume the channel is constant over the entire frame. The transmitted code matrix has the

form

$$\mathbf{S} = \begin{bmatrix} \mathbf{P} \\ \mathbf{D} \end{bmatrix},$$

where  $\mathbf{P}$  represents pilot blocks which are known at the receiver, and  $\mathbf{D}$  represents data blocks. The received vector has the form

$$\mathbf{R} = \begin{bmatrix} \mathbf{R}_p \\ \mathbf{R}_d \end{bmatrix},$$

where  $\mathbf{R}_p$  is the received pilot block and  $\mathbf{R}_d$  is the received data block. The optimal receiver can be expressed as

$$\max_{\mathbf{D}} 2\Re(\mathbf{R}_d^H \mathbf{D} \mathbf{P}^H \mathbf{R}_p) - \mathbf{R}_d^H \mathbf{D} \mathbf{D}^H \mathbf{R}_d.$$

Furthermore, suppose  $\mathbf{D}$  has the form

$$\mathbf{D} = \begin{bmatrix} \mathbf{D}_1 \\ \mathbf{D}_2 \\ \vdots \\ \mathbf{D}_{B_d} \end{bmatrix},$$

where  $\mathbf{D}_i$  is the  $i^{\text{th}}$  transmitted code matrix and  $B_d$  is the number data blocks transmitted in a frame. Also, suppose

$$\mathbf{R}_d = \begin{bmatrix} \mathbf{R}_{d,1} \\ \mathbf{R}_{d,2} \\ \vdots \\ \mathbf{R}_{d,B_d} \end{bmatrix}.$$

Then the optimal receiver has the form

$$\max_{\mathbf{D}} \Re \left( \mathbf{R}_{d,1}^H \mathbf{D}_1 \hat{\mathbf{H}} + \sum_{i=2}^{B_d} \mathbf{R}_{d,i} \mathbf{D}_i \left( \hat{\mathbf{H}} - \sum_{j=1}^{i-1} \mathbf{D}_j^H \mathbf{R}_{d,j} \right) \right), \quad (3.35)$$

where  $\hat{\mathbf{H}} = \mathbf{P}^H \mathbf{R}_p$ . Notice the optimal receiver must jointly detect all code blocks,  $\mathbf{D}_i$ .

A simpler sub-optimal detector is given by

$$\max_{\mathbf{D}_i} \Re \left( \mathbf{R}_{d,i}^H \mathbf{D}_i \hat{\mathbf{H}} \right). \quad (3.36)$$

This detector uses the pilot block to estimate the channel with  $\hat{\mathbf{H}}$  and afterward assumes this is the exact channel. From (3.35) it is clear this is not an optimal scheme because it does not take advantage of the data itself to help estimate the channel. Also notice each code block has been decoupled, and since the code is orthogonal, each symbol can be decoupled, as in (3.24).

## CHAPTER IV

## PERFORMANCE

Performance of the class I and class II non-linear orthogonal codes are presented in Section A and B, respectively. For a fair comparison of all simulations, the symbol energy,  $E$ , is normalized by a factor of  $\eta/N_t$ . Thus, the total energy emitted per bit is the same for all schemes regardless of the number of transmit antennas. Recall that the channel is modeled with quasi-static fading, in which fading is constant within a space-time code block and changes independently between blocks.

Most of the following simulation plots compare the new code performance against ML performance of Papadias' code [23], the ABBA code [21], the rate 1/2 STTD orthogonal design [3], the constellation rotating code [27, 28], and STTD-OTD [25] defined in (3.1). Unless otherwise stated, receivers have perfect knowledge of the channel. Also, most simulations transmit 2 bits/sec/Hz with QPSK for rate 1 codes, and 16QAM for the rate 1/2 STTD code [3]. Performance of maximal ratio combining (MRC) is also presented with SNR normalized by a factor of 6 dB ( $N_t = 4$ ). This curve represents a performance goal analogous to MRC compared with the Alamouti code in the two transmit antenna case.

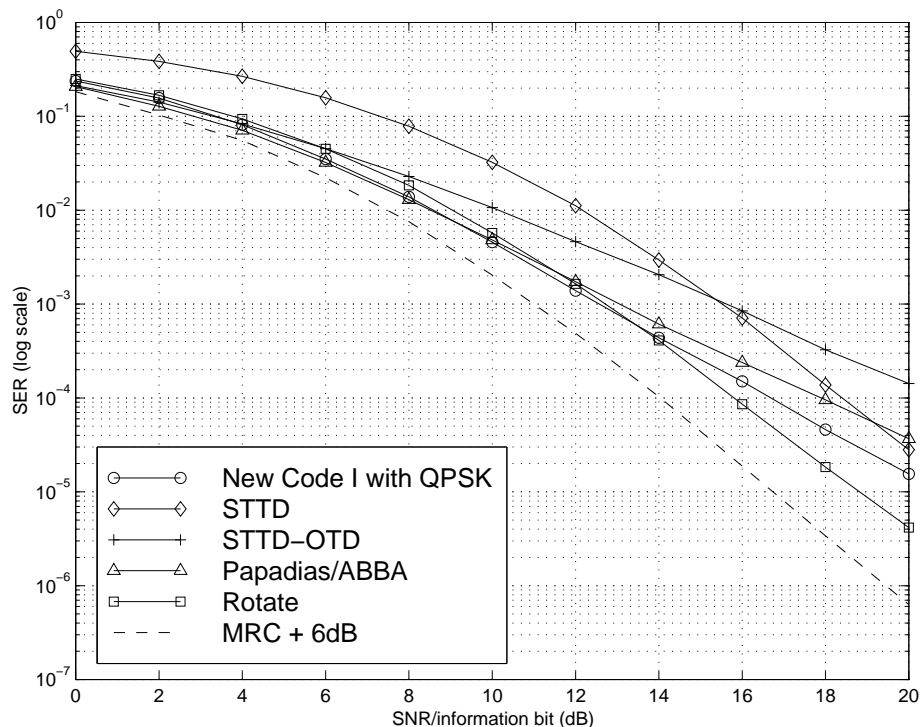


Fig. 7. ML performance of the class I non-linear code with QPSK base symbols and no phase shifts.

#### A. Class I Non-Linear Code Performance

##### 1. Non-Rotated QPSK Constellations

Consider the new class I non-linear orthogonal code with unrotated QPSK symbols (spectral efficiency 2). The symbol error rate (SER) for this code and several other comparable codes are presented in Fig. 7. Observe that the new orthogonal code outperforms STTD-OTD [25] for SNR above 4 dB and Papadias' code [23] for SNR over 12 dB. Below approximately 20 dB, the new orthogonal code also performs better than the full diversity rate 1/2 STTD code proposed in [3]. Above 14 dB, the complex constellation rotating code [27], [28] performs better than any other code. From the slope of the plot, note the new code achieves a diversity order around 3.

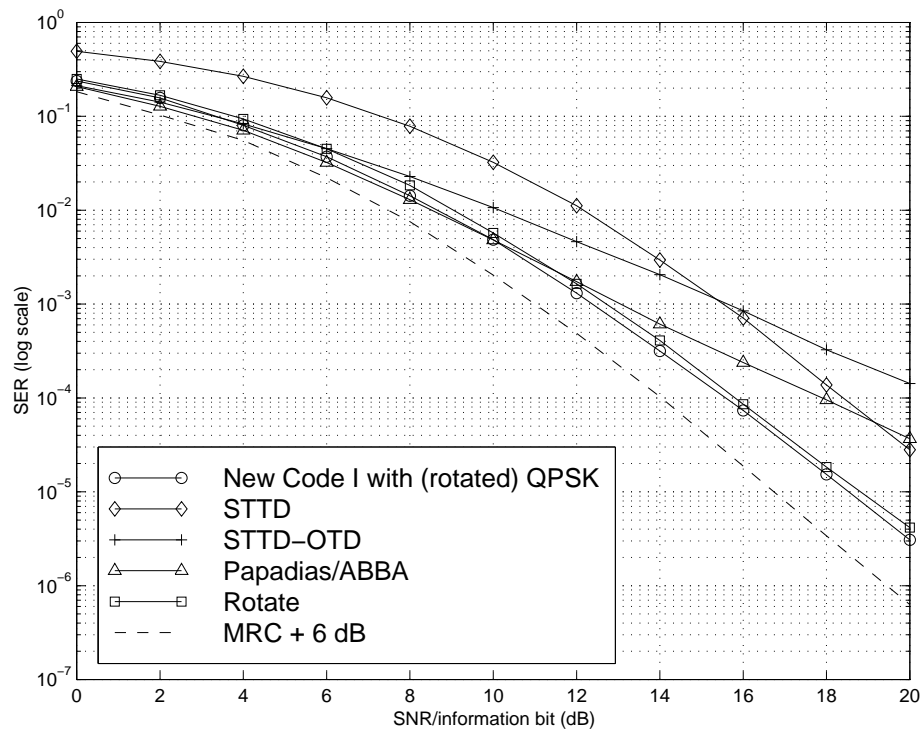


Fig. 8. ML performance of the class I non-linear code with QPSK symbols and phase shifts  $[0, 0, 32, 19] \pi/128$ .

## 2. Rotated QPSK Constellations

Using the phase rotation  $[0, 0, 32, 19] \pi/128$ , the new class I non-linear orthogonal code has full diversity with QPSK symbols. The code SER is presented in Fig. 8 with other 4 transmit antenna codes using 2 bits/sec/Hz. The performance of the new code has drastically improved from only a simple constellation phase rotation. It is now slightly better than the complex constellation rotating code [27], [28] for all SNR values. However, below 10 dB, Papadias' code [23] (and equivalent ABBA code [21]) are slightly better than the new code.

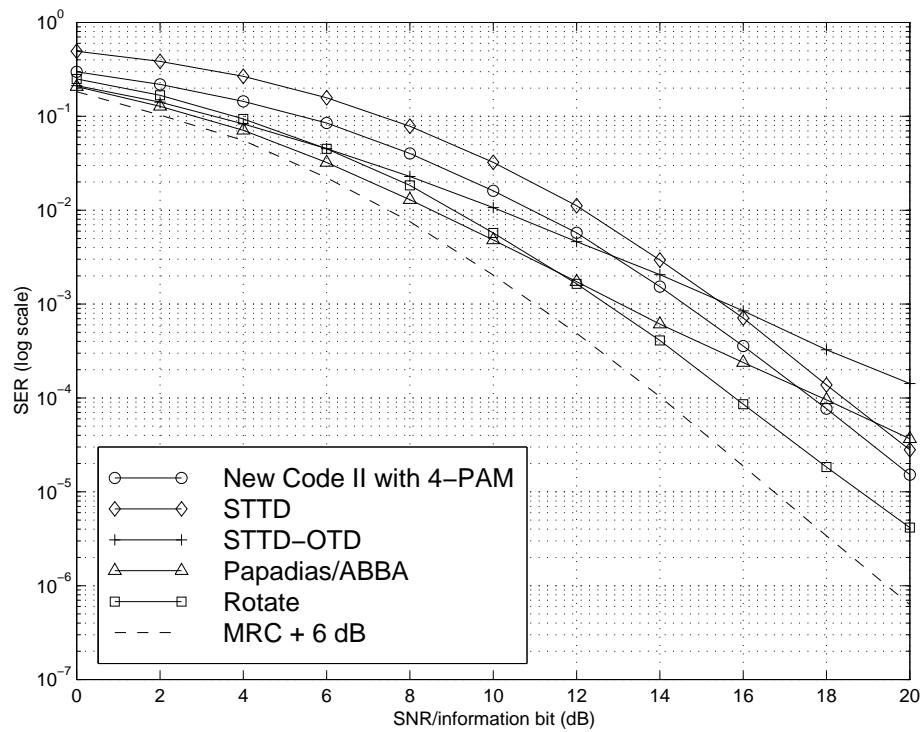


Fig. 9. ML performance of the orthogonal code with 4PAM base symbols and phase shifts  $[0, 1, 0, 1] \pi/2$ .

## B. Class II Non-linear Code Performance

### 1. Rotated 4-PAM Constellations

Consider the new class II non-linear orthogonal code with rotated 4-PAM symbols, having an overall spectral efficiency of 2 bits/sec/Hz. The SER for this and several other comparable codes are presented in Fig. 9. Recall that the new code is an orthogonal code and has a linear receiver. The new code performance exceeds that of all other transmit diversity codes with linear receivers compared. However, Papadias' code [23] and the ABBA code [21] perform better. The new code with PSK based constellations motivates the design of similar orthogonal codes with symbol constellations that have better performance.

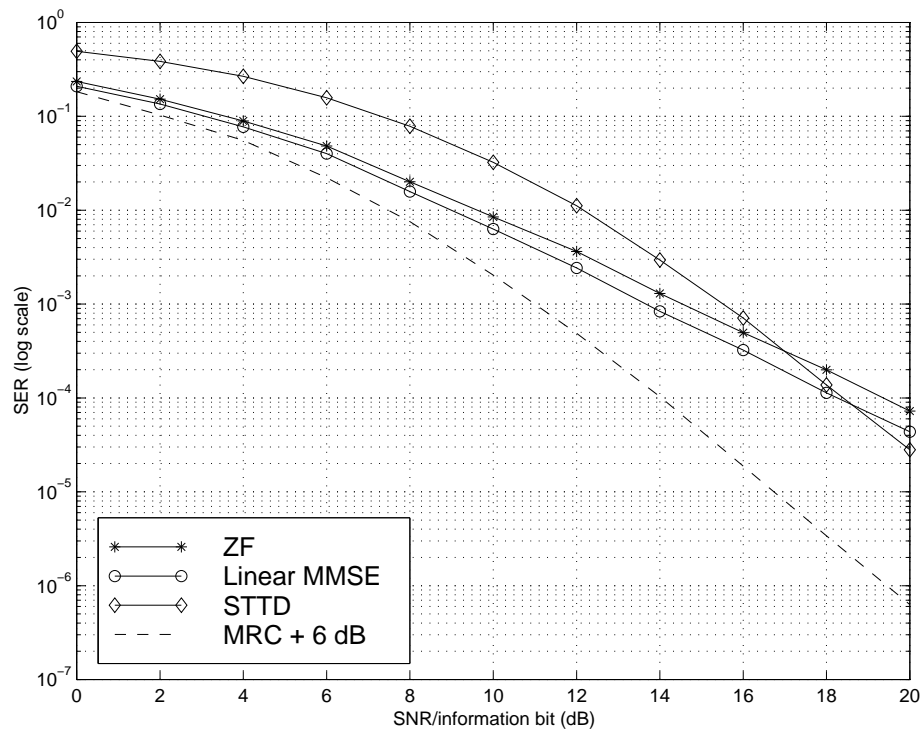


Fig. 10. ZF and linear MMSE performance of the class II non-linear code with QPSK base symbols and phase shifts  $[0, 1, 0, 1] \pi/4$ .

## 2. Rotated QPSK Constellations and Linear Receiver

Consider the new class II non-linear orthogonal code with rotated QPSK symbols, having an overall spectral efficiency of 2 bits/sec/Hz. The SER for this code and the rate 1/2 STTD orthogonal design [3] with 16QAM are presented in Fig. 10. Note all codes in the plot have linear receivers. The new code loses diversity when a sub-optimal ZF or MMSE receiver is used.

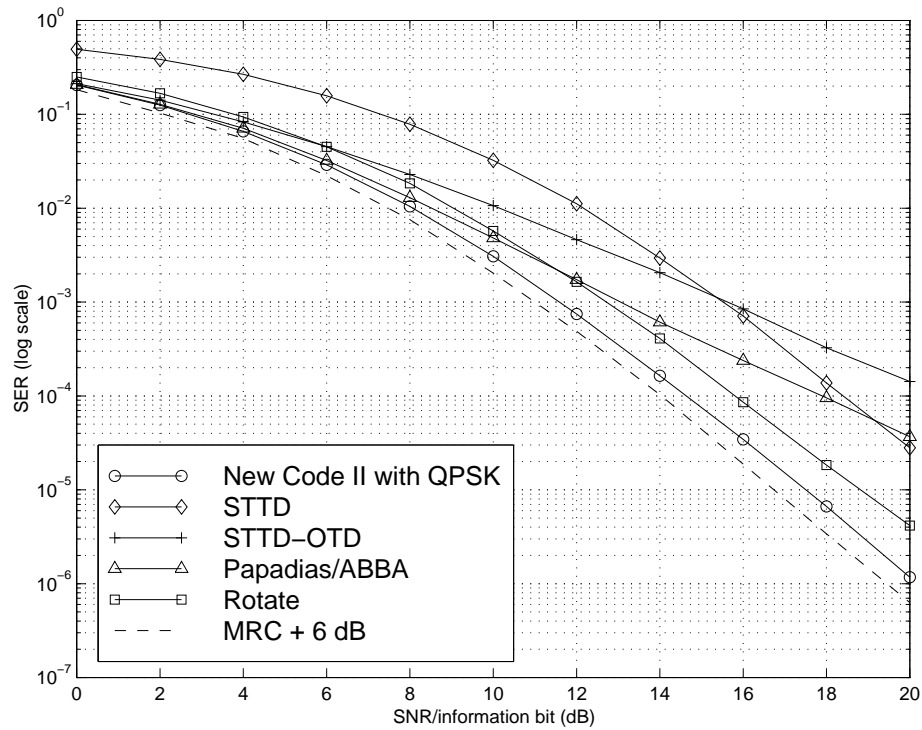


Fig. 11. ML performance of the class II non-linear code with QPSK base symbols and phase shifts  $[0, 1, 0, 1] \pi/4$ .

### 3. Rotated QPSK Constellations and ML Receiver

Consider the new class II non-linear orthogonal code with rotated QPSK symbols, having an overall spectral efficiency of 2 bits/sec/Hz. The SER for this and several other comparable codes are presented in Fig. 11. The new code outperforms all other transmit diversity codes compared. For high SNR, it has a coding gain of more than 1 dB over the next best code, and lies less than 1 dB from the MRC performance goal.

#### 4. Rotated BPSK Constellations and Unknown Fading

In this simulation, the receiver does not know the fading exactly, and uses pilot symbols to estimate it. These channel estimates are then assumed to be perfect and used to estimate the data in a frame of several space-time blocks. We assume fading is constant within a frame ( $f_m T = 0$ ). To compare different pilot symbol schemes, symbol energy is normalized by the following factor, to transmit a fixed amount of energy per information bit.

$$\frac{\text{Data Energy/frame}}{\text{Data Energy/frame} + \text{Pilot Energy/frame}}.$$

Simulations in Fig. 12 use the sub-optimal receiver in (3.36) with the class II non-linear orthogonal code and BPSK based symbols. Note this is an orthogonal code. Performance of the code with known fading is also shown for comparison. Note performance of the code is severely degraded when the channel is unknown. The best pilot insertion rate shown is 4/14, which is about 3 dB away from the known fading curve. Performance does not always improve when using more pilot blocks because additional pilots must use energy that would have been allocated to data blocks. As more pilots are added, they do not improve the fading estimate enough to compensate for the energy normalization.

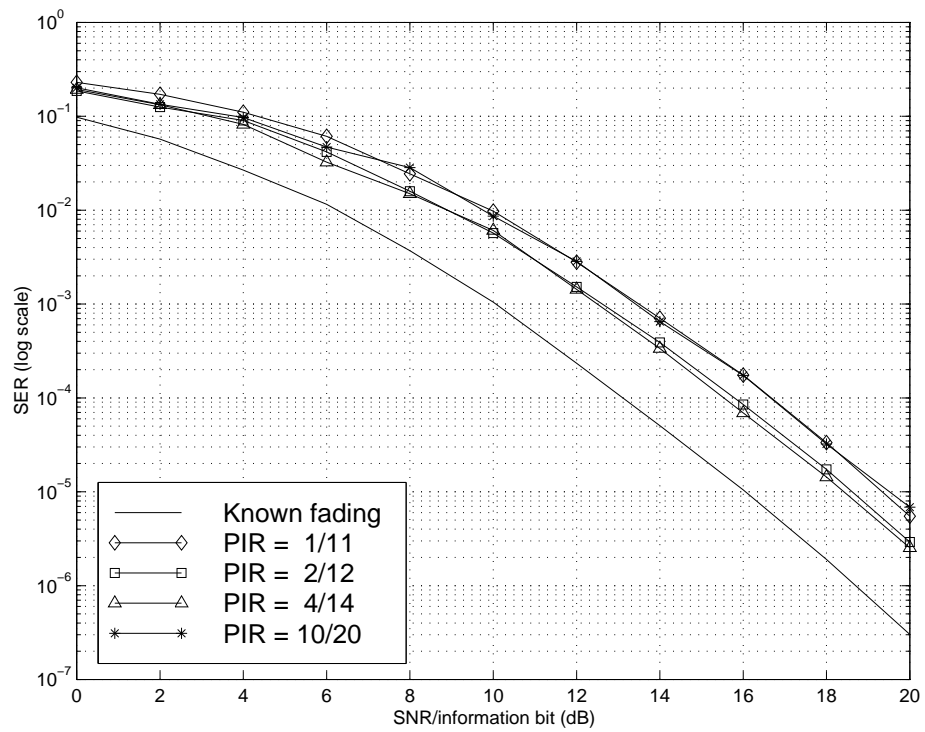


Fig. 12. Sub-optimal performance in unknown fading ( $f_m T = 0$ ) of the class II non-linear code with BPSK base symbols and phase shifts  $[0, 1, 0, 1] \pi/2$ .

## CHAPTER V

## CONCLUSION

## A. Summary of Results

In Chapter 2, we designed a class I non-linear orthogonal code. The new code with BPSK constellations proves that linear complex square orthogonal codes with full rate and full diversity can exist for *specific* constellations. Also in the analysis of this code, we have seen that rotating symbol constellations is a useful tool to improve diversity.

In Chapter 3, a class II non-linear orthogonal code was then presented. We showed this code has a receiver with moderate complexity, which can decouple symbols into pairs. In general, the new code does not achieve full diversity, but using constellation phase rotations we showed that full diversity is easily attained. The performance of the new code with rotated PSK based constellations is excellent compared with other 4 transmit antenna space-time block codes.

From the new class II non-linear orthogonal code of Chapter 3, we created square, orthogonal, full rate and full diversity space-time code for 4 transmit antennas with complex  $M$ -PAM based constellations. At first, it appears the new code with PAM base symbols violates the Hurwitz-Radon theorem. However, this theorem has a subtle limitation that is commonly overlooked. It states that square complex orthogonal designs with full rate and diversity cannot exist, meaning that a general code cannot exist for all possible symbol constellations. However, one may exist for a specific restricted constellation. For example, note when complex symbols are confined to the real line (i.e., for real symbols), orthogonal designs exist for 4 and 8 transmit antennas. The new orthogonal code with PAM symbols is significant as an existence

result, and motivates the search for similar codes with better performance.

A code that is only orthogonal or only has full diversity for specific constellations is still very practical. The desired data rate of a communication system is typically known, allowing a system designer to customize a full rate, full diversity code tailored to meet his specifications.

## B. Future Work

The next step in our research is to extend the proposed class II non-linear orthogonal code to more than 4 transmit antennas. Using these generalized codes as an example, we will explore and study the existence of linear orthogonal codes using confined constellation sets. Once these codes are better understood, we can focus on designing codes with better performance, or possibly developing a useful design criteria.

In this thesis we showed that symbol phase rotations are a useful tool to improve diversity. This has been noted from many codes, including constellation rotating codes [27]–[29], for example. These codes are actually class II non-linear orthogonal codes, and also use constellation phase rotations to attain full diversity. An interesting direction for research is to study constellation rotations or FSM design techniques to increase diversity for space-time codes. As a preliminary experiment, we found Papadias' code [23], a non-orthogonal code which nearly achieves capacity and has an elegant sub-optimal linear receiver, can achieve full diversity with rotated QPSK symbols.

Finally, it is known that full rate delay-optimal orthogonal codes (codes with minimum  $T$  for a given rate and  $N_t$ ) are not square unless  $N_t = 2$ . Designing full rate non-square orthogonal codes for  $N_t > 2$  remains an interesting problem.

## REFERENCES

- [1] W. C. Jakes, Ed., *Microwave Mobile Communications*, New York: Wiley, 1974.
- [2] G. L. Stuber, *Principles of Mobile Communication*, Norwell, MA: Kluwer Academic Publishers, 2nd ed., 2001.
- [3] V. Tarokh, H. Jafarkhani and A. R. Calderbank, "Space-time block codes for orthogonal designs," *IEEE Trans. Inform. Theory*, vol. 45, pp. 1456–1466, July 1999.
- [4] V. Tarokh, N. Seshadri and A. R. Calderbank, "Space-time codes for high data rate wireless communication: performance criterion and code construction," *IEEE Trans. Inform. Theory*, vol. 44, pp. 744–765, Mar. 1998.
- [5] B. M. Hochwald and W. Sweldens, "Differential unitary space-time modulation," *IEEE Trans. Commun.*, vol. 48, pp. 2041–2052, Dec. 2000.
- [6] G. J. Foschini and M. J. Gans, "On limits of wireless communication in a fading environment when using multiple antennas," *Wireless Personal Commun.*, vol. 6, pp. 311–335, Mar. 1998.
- [7] I. E. Telatar, "Capacity of multi-antenna Gaussian channels," *AT&T Bell Laboratories Internal Tech. Memo.*, June 1995.
- [8] J. G. Foschini, "Layered space-time architecture for wireless communication in a fading environment when using multi element antennas," *Bell Labs Tech. J.*, vol. 2, pp. 41–59, Autumn 1996.
- [9] A. Wittenben, "Base station modulation diversity for digital SIMULCAST," in *Proc. IEEE Vehicular Tech. Conf. (VTC)*, St. Louis, MO, May 1991, pp. 848–853.

- [10] A. Wittenben, “A new bandwidth efficient transmit antenna modulation diversity scheme for linear digital modulation,” in *Proc. IEEE Int. Conf. Commun. (ICC)*, Geneva, Switzerland, May 1993, pp. 1630–1634.
- [11] N. Seshadri and J. H. Winters, “Two signaling schemes for improving the error performance of FDD transmission systems using transmitter antenna diversity,” in *Proc. IEEE Vehicular Tech. Conf. (VTC)*, Secaucus, NJ, May 1993, pp. 508–511.
- [12] J. H. Winters, “The diversity gain of transmit diversity in wireless systems with Rayleigh fading,” in *Proc. IEEE Int. Conf. Commun. (ICC)*, New Orleans, LA, May 1994, vol. 2, pp. 1121–1125.
- [13] A. R. Hammons and H. E. Gamal, “On the theory of space-time codes for PSK modulation,” *IEEE Trans. Inform. Theory*, vol. 46, pp. 524–542, Mar. 2000.
- [14] S. M. Alamouti, “A simple transmit diversity technique for wireless communications,” *IEEE J. Select Areas Commun.*, vol. 16, pp. 1451–1458, Oct. 1998.
- [15] V. Tarokh, H. Jafarkhani and A. R. Calderbank, “Space-time block coding for wireless communications: performance results,” *IEEE J. Select Areas Commun.*, vol. 17, pp. 451–460, Mar. 1999.
- [16] G. Ganesan and P. Stoica, “Space-time diversity using orthogonal and amicable orthogonal designs,” in *Proc. IEEE Int. Conf. Acoust., Speech, Signal Processing (ICASSP)*, Istanbul, Turkey, June 2000, pp. 2561–2564.
- [17] O. Tirkkonen and A. Hottinen, “Complex space-time block codes for four Tx antennas,” in *GLOBECOM Conf. Records*, San Francisco, CA, Nov.–Dec. 2000, vol. 2, pp. 1005–1009.

- [18] B. M. Hochwald, T. L. Marzetta and C. B. Papadias, “A novel space-time spreading scheme for wireless CDMA systems,” in *Proc. 37th Annual Allerton Conf. on Commun. Control, and Computing*, Monticello, IL, Sept. 1999, pp. 1284–1293.
- [19] L. A. Dalton and C. N. Georghiades, “A Four Transmit Antenna Orthogonal Space-Time Code with Full Diversity and Rate,” in *Proc. 40th Annual Allerton Conf. on Commun. Control, and Computing*, Monticello, IL, Oct. 2002.
- [20] B. M. Hochwald and T. L. Marzetta, “Unitary space-time modulation for multiple-antenna communications in Rayleigh flat fading,” *IEEE Trans. Inform. Theory*, vol. 46, pp. 543–564, Mar. 2000.
- [21] O. Tirkkonen, A. Boariu and A. Hottinen, “Minimal non-orthogonality rate 1 space-time block code for 3+ Tx,” in *IEEE Int. Symposium on Spread Spectrum Techniques & Applications*, New Jersey, USA, Sept. 2000, pp. 429–432.
- [22] H. Jafarkhani, “A quasi-orthogonal space-time block code,” *IEEE Trans. Commun.*, vol. 49, pp. 1–4, Jan. 2001.
- [23] C. B. Papadias and G. J. Foschini, “A space-time coding approach for systems employing four transmit antennas,” in *Proc. IEEE Int. Conf. Acoust., Speech, Signal Processing (ICASSP)*, Salt Lake City, Utah, May 2001, pp. 2481–2484.
- [24] A. Yongacoglu and M. Siala, “Performance of diversity systems with 2 and 4 transmit antennas,” in *Proc. Int. Conf. Commun. Tech. (WCC-ICCT)*, Peking, China, 2000, pp. 148–150.
- [25] L. M. A. Jalloul, K. Rohani, K. Kuchi and J. Chen, “Performance analysis of CDMA transmit diversity methods,” in *Proc. IEEE Vehicular Tech. Conf. (VTC)*, Amsterdam, Netherlands, Oct. 1999, vol. 3, pp. 1326–1330.

- [26] M. O. Damen, K. Abed-Meraim and J. C. Belfiore, "Transmit diversity using rotated constellations with Hadamard transform," in *Proc. Adaptive Systems for Signal Processing, Commun. and Control Conf.*, Lake Louise, Alberta, Canada, Oct. 2000, pp. 396-401.
- [27] Y. Xin, Z. Wang and G. B. Giannakis, "Linear unitary precoders for maximum diversity gains with multiple transmit and receive antennas," in *Proc. 34th Asilomar Conf. Signals, Systems, and Computers*, Pacific Grove, CA, Oct.–Nov. 2000, pp. 1553–1557.
- [28] Y. Xin, Z. Wang and G. B. Giannakis, "Space-time diversity systems based on unitary constellation-rotating precoders," in *Proc. IEEE Int. Conf. Acoust., Speech, Signal Processing (ICASSP)*, Salt Lake City, Utah, May 2001, pp. 2429–2432.
- [29] V. M. DaSilva and E. S. Sousa, "Fading-resistant modulation using several transmitter antennas," *IEEE Trans. Commun.*, vol. 45, pp. 1236–1244, Oct. 1997.
- [30] S. Rouquette, S. Mériegeault and K. Gosse, "Orthogonal full diversity space-time block coding based on transmit channel state information for 4 Tx antennas," in *Proc. IEEE Int. Conf. Commun. (ICC)*, New York City, NY, April–May 2002, vol. 1, pp. 558–562.

## APPENDIX A

## FAILING MATRIX PAIRS WITH PHASE SHIFTS

Using the new class I non-linear orthogonal code with QPSK symbols having counter-clockwise phase shifts  $[0, 1, 2, 3] \pi/16$ , the number of failing matrix pairs was reduced to 64 from 384. Of these 64 pairs, each contained at least one of the 32 code matrices from Table I. Thus, by excluding these “bad” matrices, the code can achieve full diversity.

The symbol constellations are shown in Fig. 13. Table I contains a list of symbol indices for bad matrices. The symbols in Table I are defined as follows: 1, 2, 3, and 4 represent the constellation points going counter-clock wise around the rotated QPSK constellation. The “total phase” column contains the sum of the four symbol phases. Notice the total phase is always  $3\pi/8$  or  $\pi + 3\pi/8$ .

Table I. “Bad” matrices for the class I non-linear code with QPSK symbols, phase shifted by  $[0, 1, 2, 3] \pi/16$ .

$s_1$	$s_2$	$s_3$	$s_4$	Total Phase	$s_1$	$s_2$	$s_3$	$s_4$	Total Phase
2	1	1	4	$3\pi/8$	4	1	1	2	$3\pi/8$
2	1	2	1	$\pi + 3\pi/8$	4	1	2	3	$\pi + 3\pi/8$
2	1	4	3	$\pi + 3\pi/8$	4	1	4	1	$\pi + 3\pi/8$
2	1	3	2	$3\pi/8$	4	1	3	4	$3\pi/8$
2	2	1	1	$\pi + 3\pi/8$	4	2	1	3	$\pi + 3\pi/8$
2	2	2	2	$3\pi/8$	4	2	2	4	$3\pi/8$
2	2	4	4	$3\pi/8$	4	2	4	2	$3\pi/8$
2	2	3	3	$\pi + 3\pi/8$	4	2	3	1	$\pi + 3\pi/8$
2	4	1	3	$\pi + 3\pi/8$	4	4	1	1	$\pi + 3\pi/8$
2	4	2	4	$3\pi/8$	4	4	2	2	$3\pi/8$
2	4	4	2	$3\pi/8$	4	4	4	4	$3\pi/8$
2	4	3	1	$\pi + 3\pi/8$	4	4	3	3	$\pi + 3\pi/8$
2	3	1	2	$3\pi/8$	4	3	1	4	$3\pi/8$
2	3	2	3	$\pi + 3\pi/8$	4	3	2	1	$\pi + 3\pi/8$
2	3	4	1	$\pi + 3\pi/8$	4	3	4	3	$\pi + 3\pi/8$
2	3	3	4	$3\pi/8$	4	3	3	2	$3\pi/8$

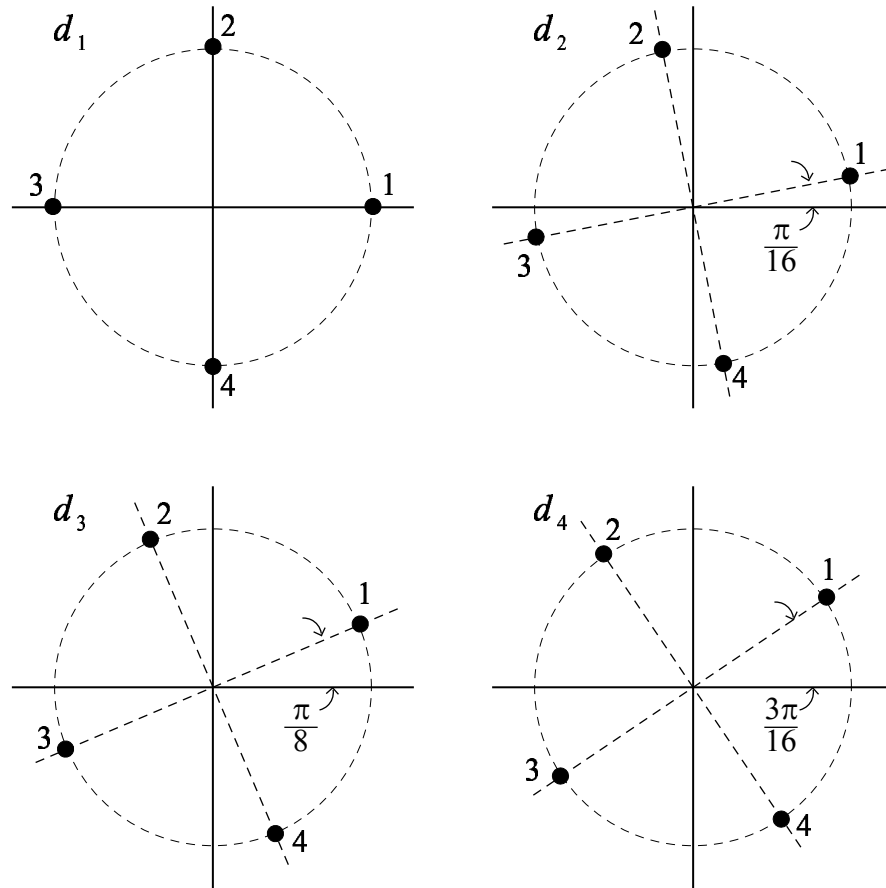


Fig. 13. QPSK symbol constellations with phase shifts  $[0, 1, 2, 3] \pi/16$ .

## VITA

Lori A. Dalton was born in Homestead, FL in 1982. She received her B.S. and M.S. degrees in electrical engineering from Texas A&M University in 2001 and 2002, respectively. She is currently a Ph.D. student under Dr. Costas N. Georghiades in the Wireless Communications Laboratory at Texas A&M University.

Upon admittance to Texas A&M, Ms. Dalton was a recipient of the Texas A&M Lechner Fellowship in August 1999. She later received TxTEC scholarships in January 2000 and September 2000, a Nokia scholarship in February 2000, and a Nortel scholarship in September 2000. She was awarded the Fouraker Graduate Fellowship and a departmental scholarship in January 2001, and an NSF Graduate Research Fellowship in March 2001. On November 3, 2001, she was announced Aggie of the Week during an A&M football game.

In 1998, she worked as a Junior Laureate summer researcher in the DNA Department at the Houston Advanced Research Center in The Woodlands, TX. In the summer of 2001, she worked in the Wireless Communications Group at Texas Instruments in Dallas, TX. She was also a member of the 2001 Future Energy Challenge A&M team, which won the nationwide competition. She is a student IEEE member.

In October 2002, she co-authored a paper with Dr. Georghiades entitled, "A Four Transmit Antenna Orthogonal Space-Time Block Code with Full Diversity and Rate" in the *40th Annual Allerton Conference on Communication, Control, and Computing*.

Her areas of interest include space-time coding, wireless communications, CDMA and spread spectrum systems, OFDM, digital signal processing, and optical communications. Her mailing address is 16415 Willow Park Dr., Tomball, TX 77377. Her email is ldalton@ee.tamu.edu.

The typist for this thesis was Ms. Lori Dalton.